Grazing incidence fast atom diffraction: a new technique for in-situ monitoring of molecular beam epitaxial growth

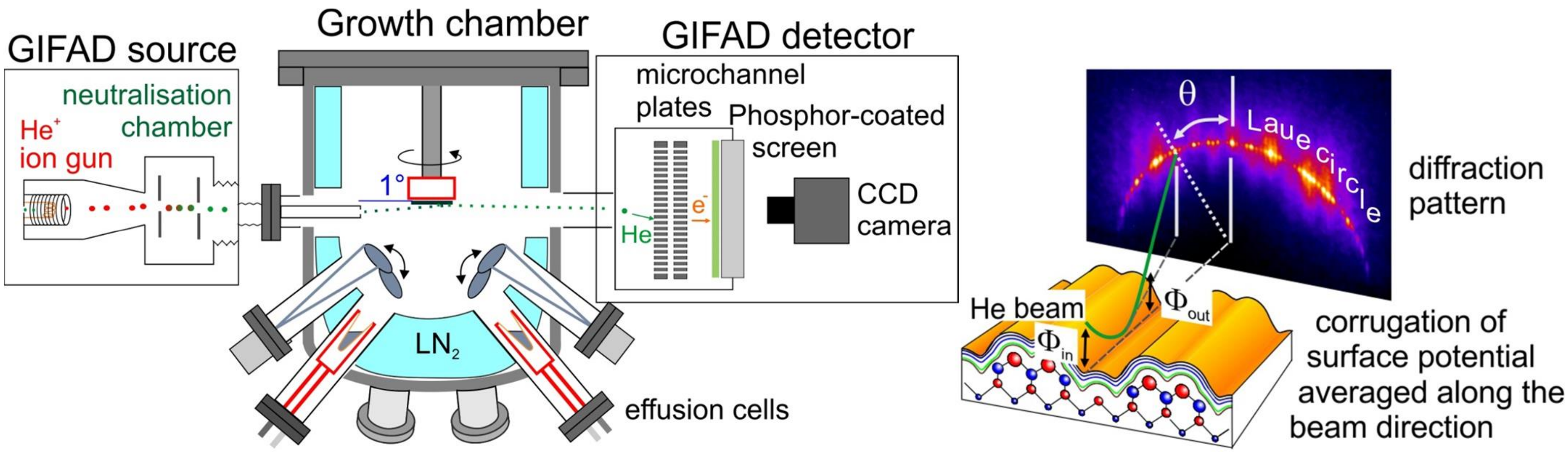

P. Atkinson
Institut des NanoSciences de Paris

Atelier « mesures in-situ pour le contrôle de la croissance épitaxiale » **GDR PULSE** 1-3 Oct 2018

Outline

- Å **Motivation and context**
- Å **Atom and ion scattering basics**
- Å **Conditions for diffraction of fast atoms**
  - Å Basic introduction to GIFAD patterns
- Å **Implementation in a conventional MBE machine**
- Å **Monitoring surfaces and growth under real growth conditions**
  - Å GaAs reconstructions and transition between reconstructions
  - Å Layer-by-layer growth
  - Å Surface sensitivity
  - Å Limitations : 3D growth monitoring
- Å **Beyond « standard » semiconductor thin film growth**
  - Å Looking at mosaicity
  - Å Alignment of van-der-Waals materials
  - Å Growth of molecular thin films
- Å **Conclusions , future challenges and open questions**

Historical Context

First demonstration of GIFAD was in 2007 on LiF by Orsay and Berlin groups (Rousseau et al, Schüller et al, PRL)

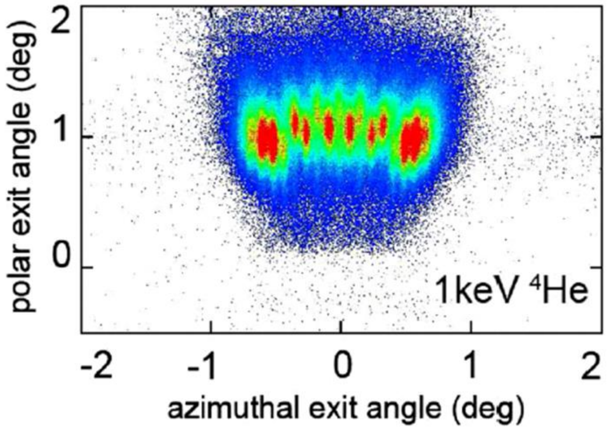

Three groups worldwide are/were recently working on developing/ understanding the GIFAD technique:

- Group of Helmut Winter (retired), Humboldt University, Berlin, Germany
- Groups of Philippe Roncin, Hocine Khemliche, ISMO, Univ. Paris-Sud Orsay (Patent holders of GIFAD)
- Group of Maria Gravielle, Universidad Buenos Aires, Argentina

GIFAD can now be bought from Scientec-Prevac.

Motivation from a growth perspective

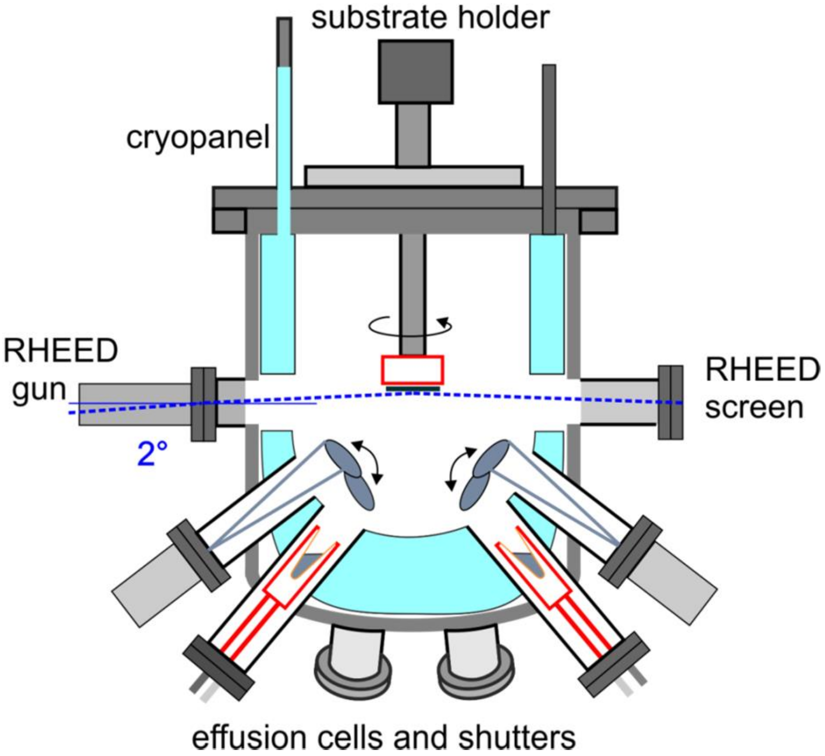

Control over thin film growth:
- Calibration of growth rate
- Determination of growth mode (2D layer-by-layer/step flow ; 3D)
- Crystal structure
- Surface quality
- Chemical composition

Diagnostic tool requirements:
- In-situ and non-invasive
- Real-time
- Quantitative interpretation

	Low energy normal incidence	High energy grazing incidence
Electrons	LEED	RHEED
Atoms, molecules	TAS	GIFAD

Easier to implement in a multi-source chamber

Greater surface sensitivity

Advantages of TAS and RHEED combined

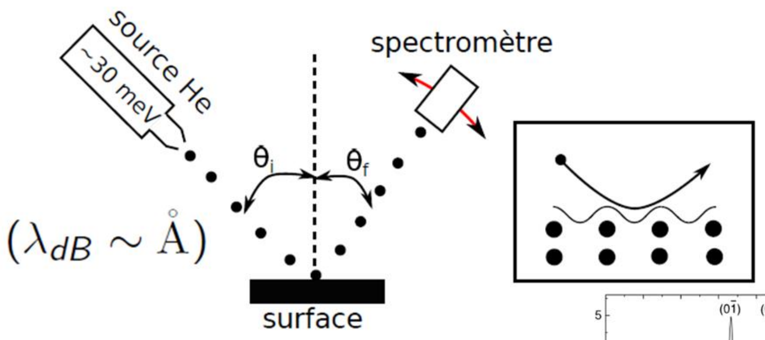

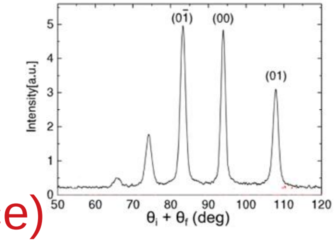

+ no penetration
(atom bounces off surface)
+ quantitative interpretation possible
- moving spectrometer (slow acquisition)
- surface needs to be cold

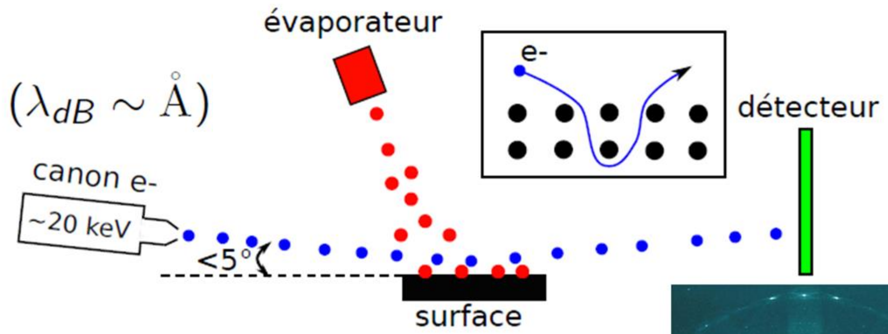

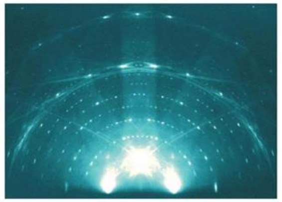

+ Simple to implement
+ Image collected on 2D detector
+ elevated substrate temperature
- penetration of electrons below surface
- multiple collisions (interpretation difficult)

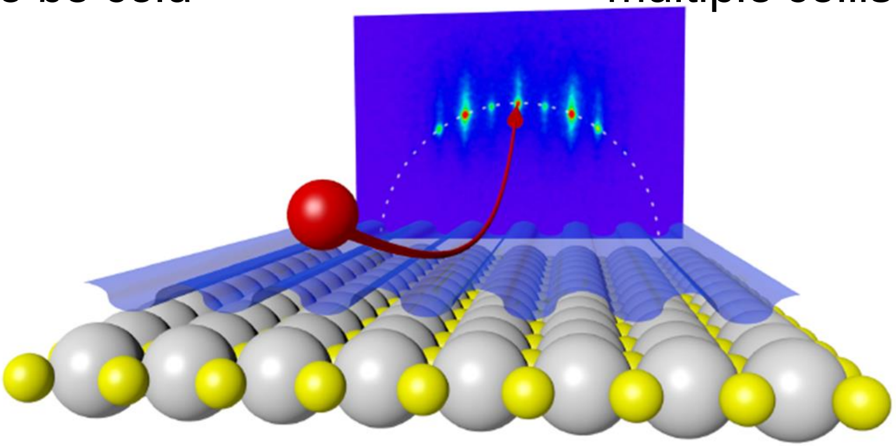

GIFAD : diffraction visible even for atomic beam energies of 5keV
$\lambda_{dB} \sim 0.2$pm

Atom/ion scattering basics

Need to think about:

- type of interaction between the probe atom/ion (in our case a He atom) and the surface
- different interaction regimes (classical, semi-classical, quantum)
- effect of surface thermal vibrations
- effect of surface defects e.g. surface steps

Atom-surface interaction

Atom-atom impact = nuclear repulsion – screening effect of the electron cloud

$$V(r) = \frac{Z_1 Z_2}{r} \qquad\qquad V(r) = \frac{Z_1 Z_2}{r} f(r)$$

Several semi-empirical choices of screening function based on Thomas -Fermi or Hartree Fock screening

➔ « Universal screening function » $f(r/a_u) = \sum_{i=1}^{4} a_i \exp(-b_i r/a_u)$

where $a_u = \frac{0{,}8853}{Z_1^{0{,}23} + Z_2^{0{,}23}}$

	i	1	2	3	4
ZBL	a_i	0,1818	0,5099	0,2802	0,02817
	b_i	3,2	0,9423	0,4028	0,2016
Molière/ OCB	a_i	0,35	0,55	0,1	0
	b_i	0,3	1,2	6	

M. Nastasi et al Ion-solid interactions: fundamentals and applications, CUP

Atom-surface interaction

Surface potential built up by superposition of pair-potentials

$$V(x,y,z) = \sum_{l=0}^{\infty} \sum_{k=-\infty}^{\infty} \sum_{j=-\infty}^{\infty} V(r_{lkj})$$

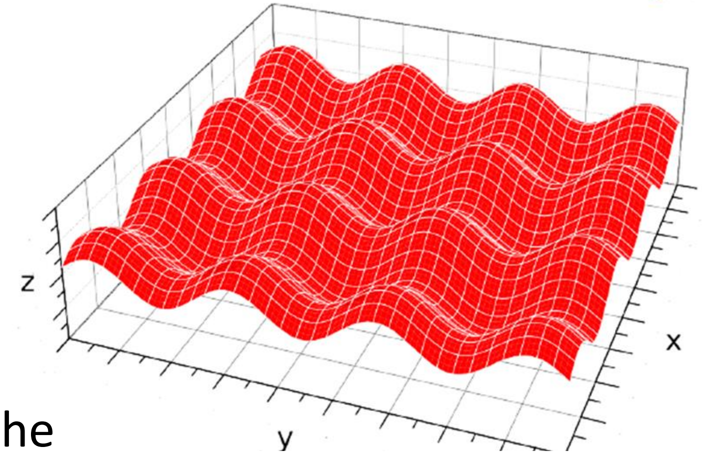

Where $V(r_{ijk})$ is the pair potential and r_{ijk} is the distance between probe atom and surface atom. The summation is only carried out over the range where the potential is valid.

This semi-empirical approach is only successful for relatively simple, ionic materials

For more complex compounds – the surface potential can be calculated by ab-initio DFT calculations, calculating the effect of a He atom approaching the surface. Pair-wise potentials for atoms on different atomic layers can then be empirically evaluated to give the same potential surface.

Grazing incidence geometry

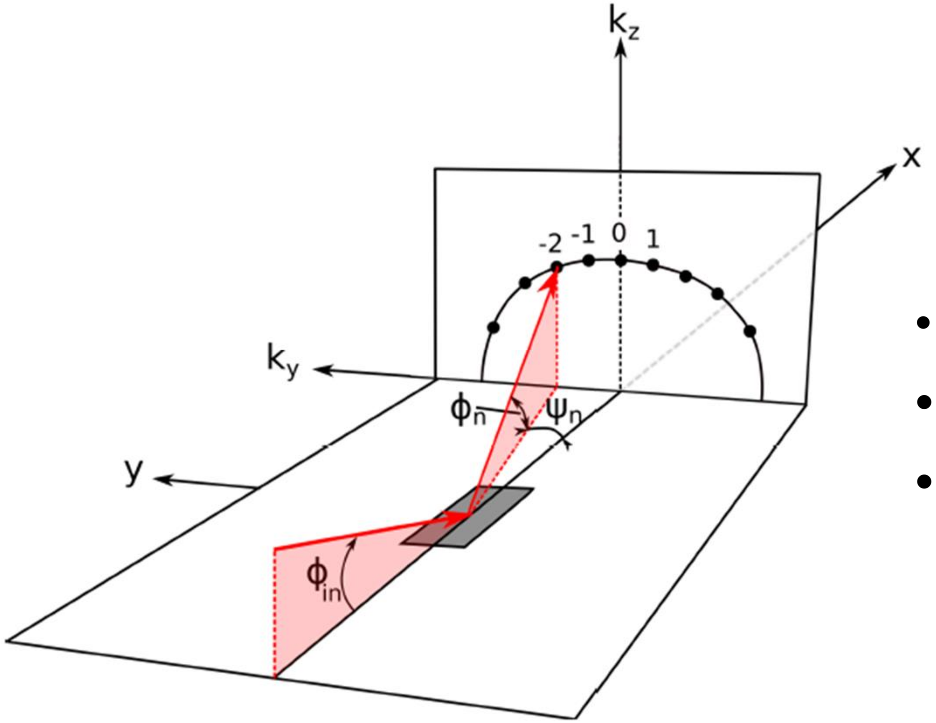

- 200eV < Ei < 5keV
- Angle of incidence ϕ in < 2°
- Diffraction spots lie on the Laue circle

Axial channeling approximation

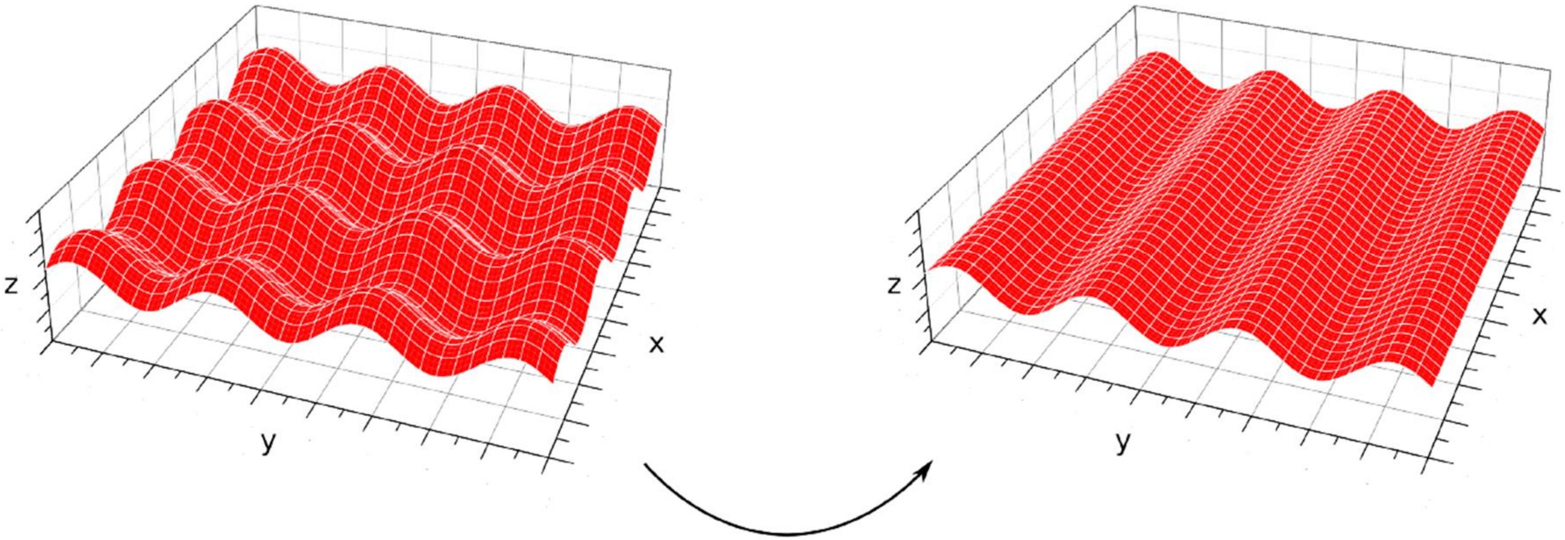

Rapid movement along x : $E_{ix} = E_i \cos^2\phi_{in} \approx E_i$ (in the range keV)
Slow movement along z : $E_{iz} = E_i \sin^2\phi_{in}$ (in the range 0.5meV – 1eV)
Channeling approximation: can consider two movements are decoupled

In the beam direction (x), the probe atom is not sensitive to surface corrugation

3D scattering problem ==> 2D scattering problem
(average of the He atom – surface potential along the rapid direction)

Corrugation function

Calculated by : adding pair potentials

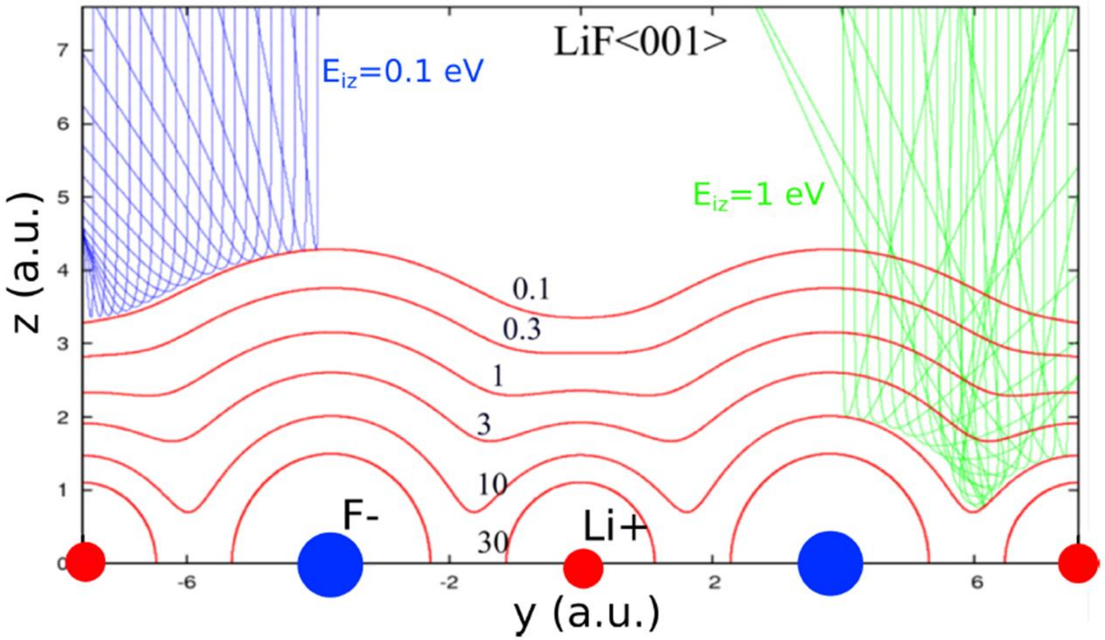

The atom of energy Eiz ťbounces offò the equipotental of the same energy

Hard wall model

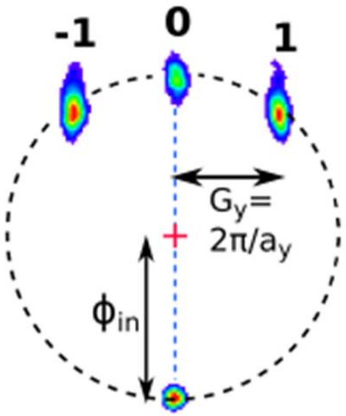

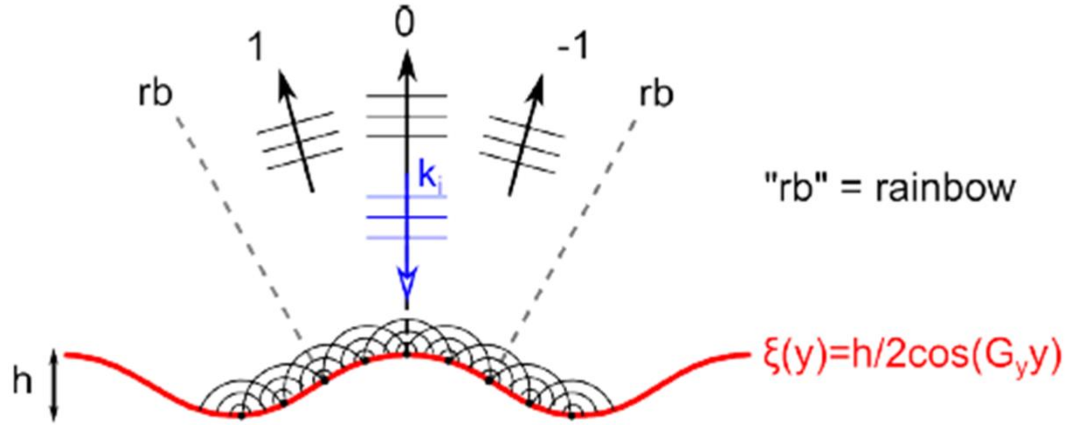

Semi-classical (Eikonal) approach :

Diffraction from the surface ≈ diffraction from a phase grating (Fourier optics)

$A_n \propto \frac{1}{d_y}\int_0^{d_y} e^{-iG_y y + i\eta} dy$ where η is the phase difference due to the surface

If the surface corrugation can be approximated by a sinusoidal function

$\eta = 2k_{iz}h\cos(G_y y)$ the diffracted intensity would be: $I_n = |A_n|^2 \propto J_n^2(hk_{iz})$

where Jn is a Bessel function

Hard wall model - disadvantages

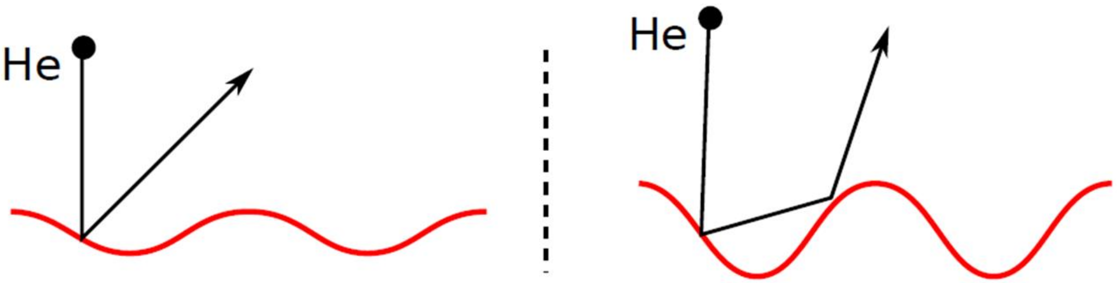

Semi-classical model can not model strongly corrugated surfaces where multiple collisions could occur

It also does not take into account van-der-Waals attraction between probe atom and surface

Solution is to use a full quantum calculation using:

- Surface potential calculated by ab-initio DFT
- Diffraction pattern calculated by wavepacket propagation
  - incident atom is described by a Gaussian wavepacket and the packet propagation is calculaed using the time-dependant Schrödinger equation

Effect of thermal vibrations

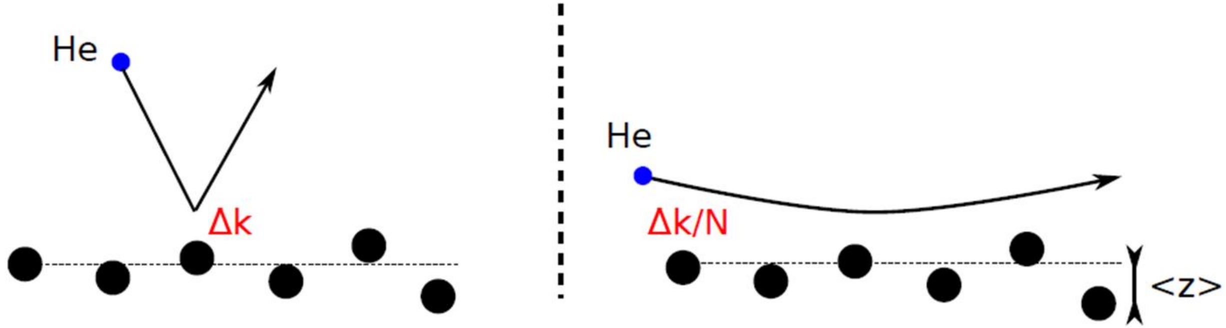

Surface atom motion modeled by a quantum harmonic oscillator

$$< z^2 >= \frac{\hbar^2 T}{2mk_B\theta_D^2}$$

For one atom collision, the Debye-Waller factor is: $e^{-2\Delta k^2 <z^2>}$

In grazing incidence the change in momentum occurs over N collision partners

i.e. Δk ➔ Δk/N $e^{-2\Delta k^2 <z^2>} \rightarrow e^{-\frac{2\Delta k^2 <z^2>}{N}}$

Diffraction is possible even at elevated substrate temperatures

Effect of steps

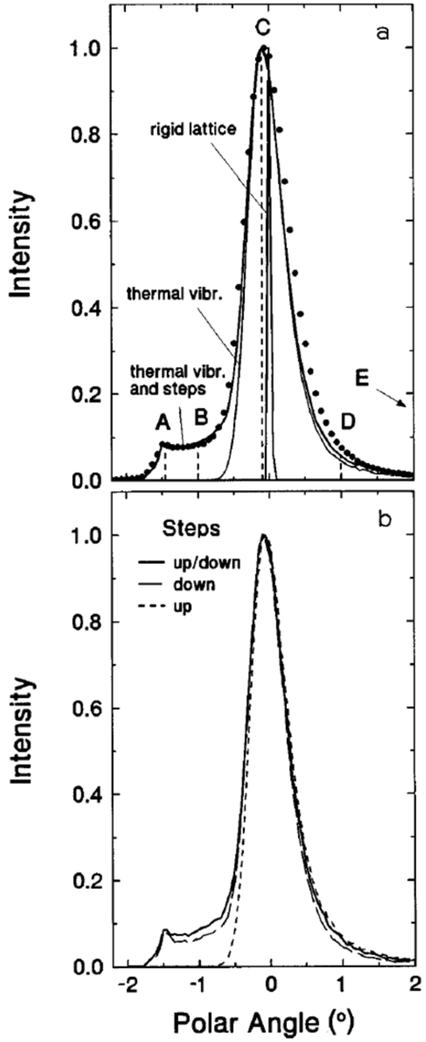

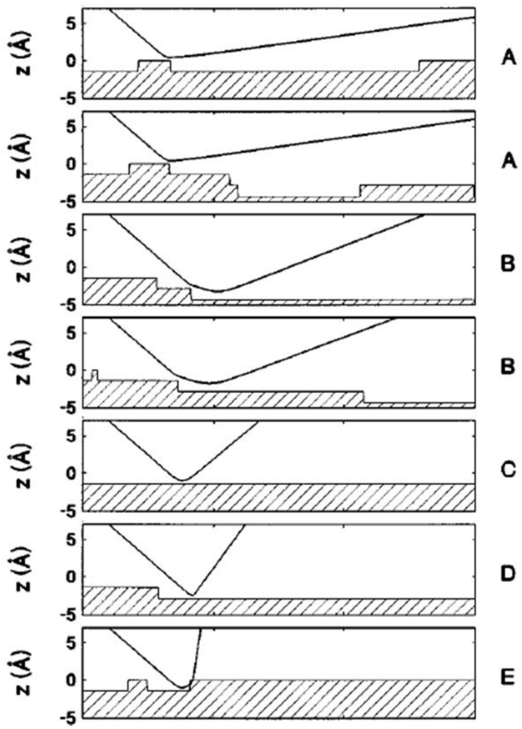

Thermal vibrations of surface lead to broadening of specular spot

Steps down ➔ subspecular scattering

Steps up ➔ superspecular scattering

See e.g Pfandzelter, PRB 57 15496 (1998)

GIFAD patterns : the basics

decoupling parallel and perpendicular motion
➔
scattering from *average* potential along incident beam

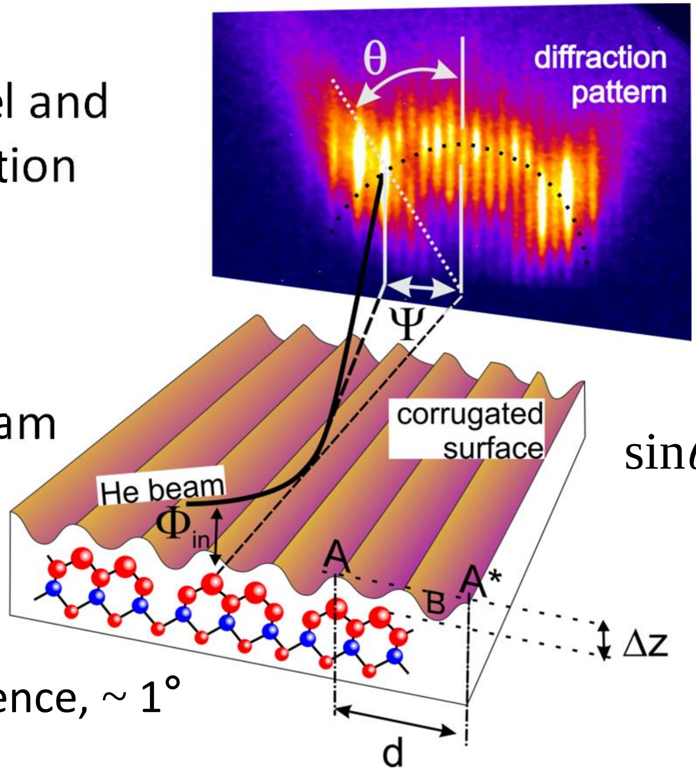

Φ_{in} : angle of incidence, ~ 1°

E_{tot}: energy of He atoms ~ 250 – 1000 eV
$E_{\perp} = E_{tot} \sin^2\Phi_{in}$ å 75 – 300 meV

$\lambda_{dB\perp}$ å 0.5 Å (c.f. λ_{dB} å 0.009 Å)
RHEED typically 12 – 20 keV, λ_{dB} å 0.1 Å

A. Schüller et al. PRL <u>98</u>, 16103 (2007)
P. Rousseau et al. PRL <u>98</u>, 16104 (2007)

Diffraction streaks (A A* interference):

$$\sin\,\theta_n = \frac{n}{d}\lambda_{dB\perp}$$

but since:

$$\sin\theta = \frac{\sin\Psi}{\sin\Phi_{in}} \quad \text{and} \quad \lambda_{dB\perp} = \lambda_{dB}\sin\Phi_{in}$$

$$\sin\,\Psi_n = \frac{n}{d}\lambda_{dB}$$

Intensity envelope (A B interference):

$$I_n = J_n^2\left(\frac{\Delta z\pi}{\lambda_{dB\perp}}\left(1+\cos\theta_n\right)\right)$$

(assuming sinusoidal hard wall)

GIFAD patterns : the basics

decreasing incident energy

$\lambda_{dB\perp}$ = 0.18 Å   0.29 Å   0.52 Å

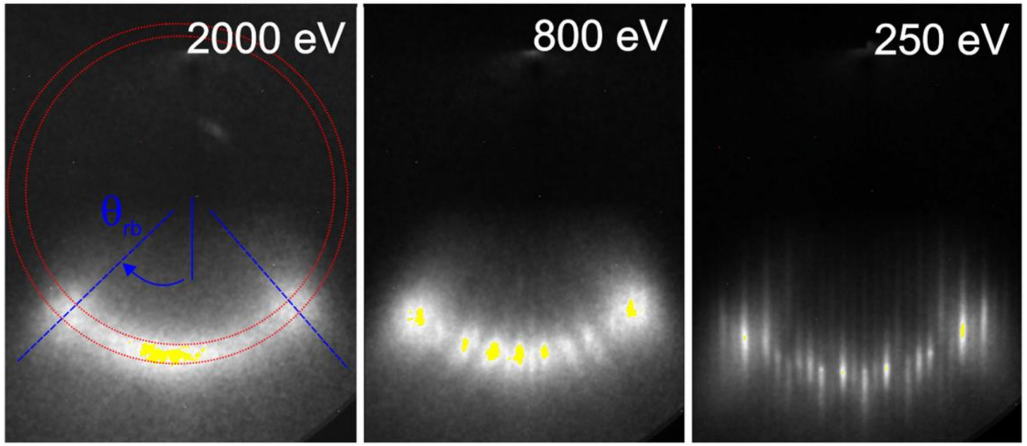

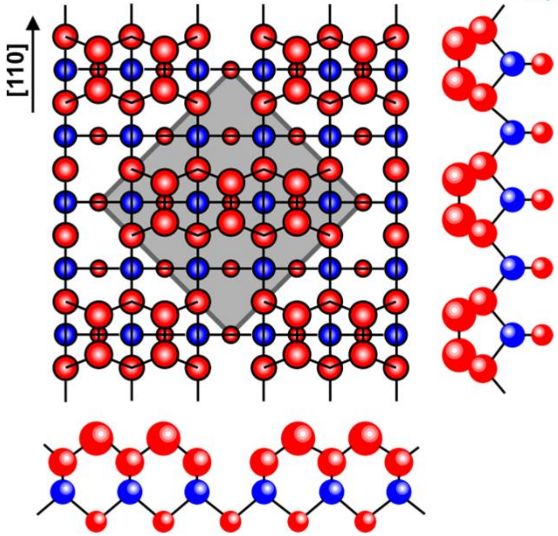

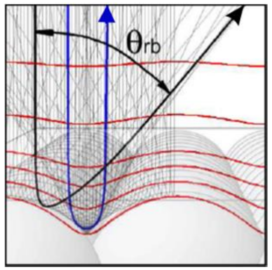

θ_{rb} = 2 arctan ($\pi\ \Delta z$ /d)

➔ Δz /d ~ 0.1

increasing incidence angle

$E_\perp$ = 5.6 meV   21 meV   51 meV   76 meV

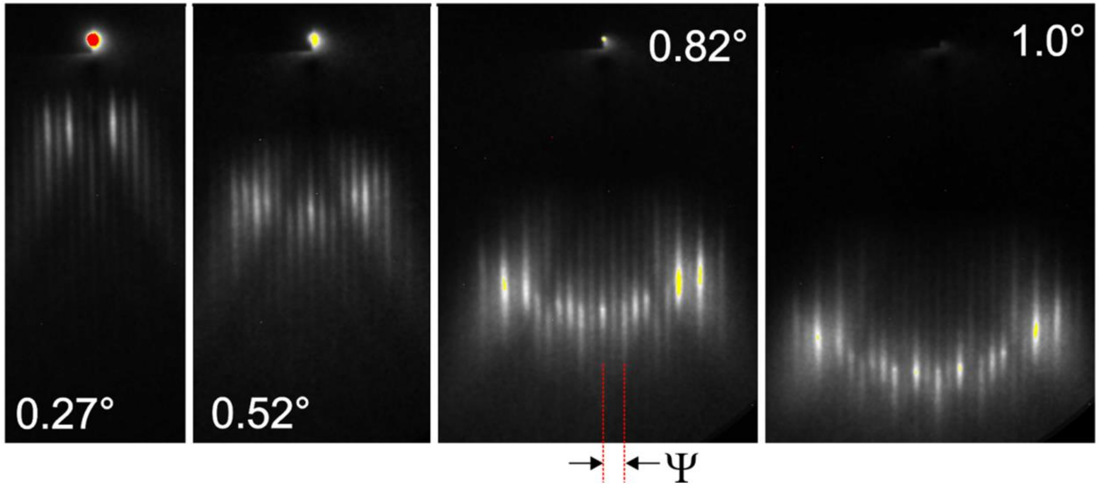

GIFAD vs. RHEED

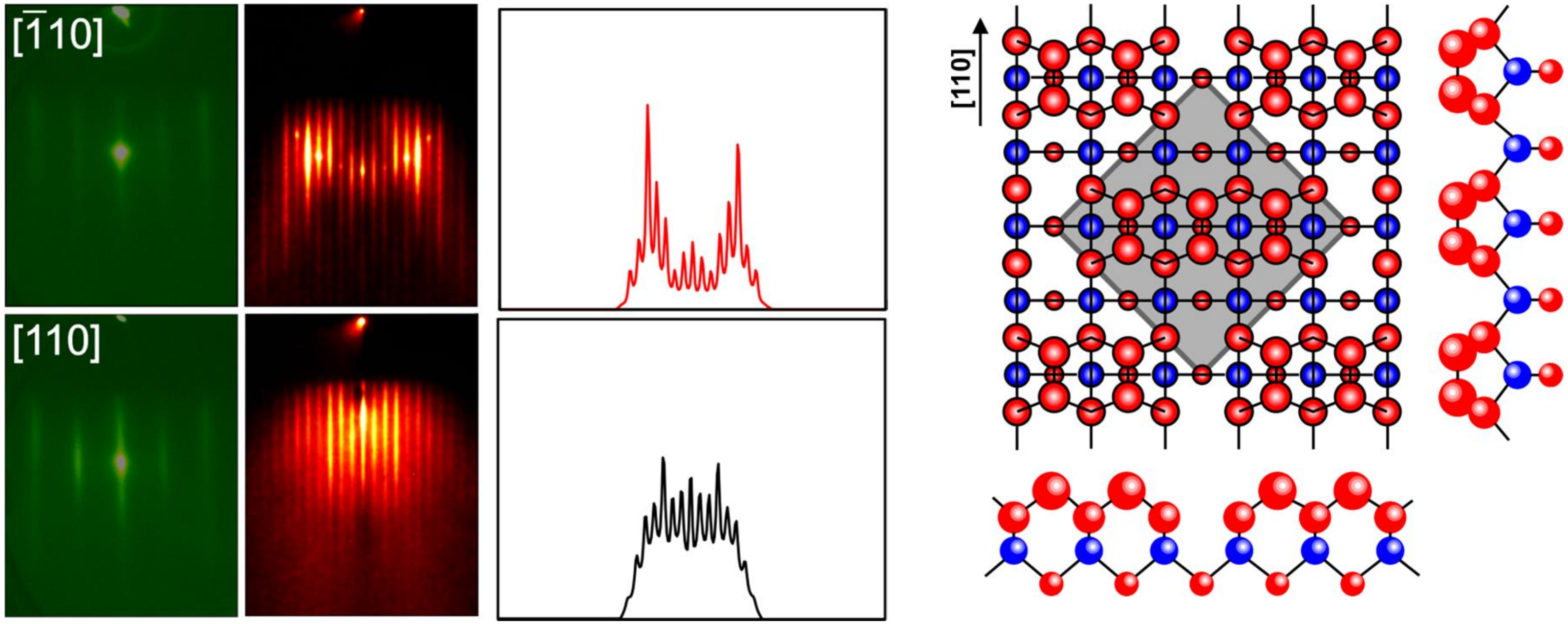

c(4×4) reconstruction:

RHEED in [110] and [-110] virtually equivalent due to square unit cell

GIFAD [110] and [-110] patterns distinguishable due to different surface corrugation

Less corrugated surface has intensity more concentrated in low diffraction orders

GIFAD vs. RHEED

GIFAD images, He at 400 eV

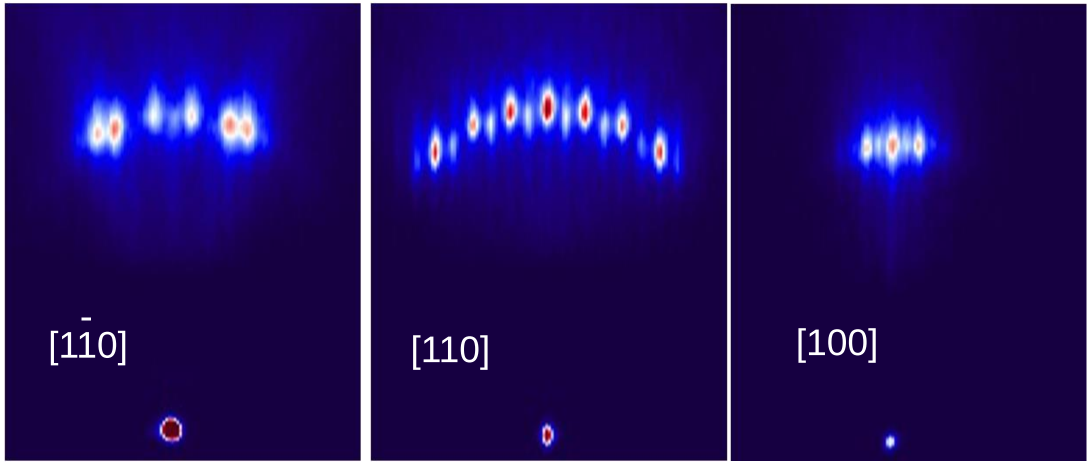

ZnSe (001) c(2x2)

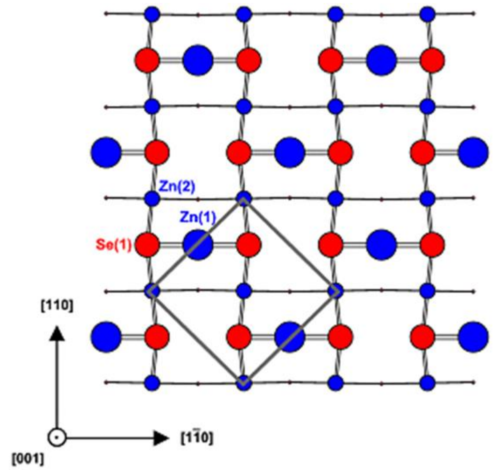

Weigand *et al.*, Phys. Rev. B **68**, 241314(2003)

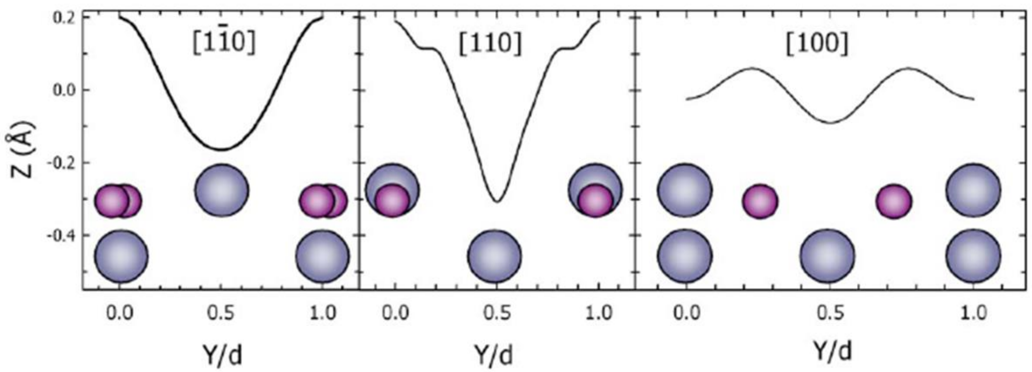

H. Khemliche and P. Roncin et al. APL 95 151901 (2009)

GIFAD sensitive to corrugation (electronic charge density)

Can directly see the charge transfer from Zn to Se in the diffraction pattern with the beam along [100]

GIFAD on an MBE chamber

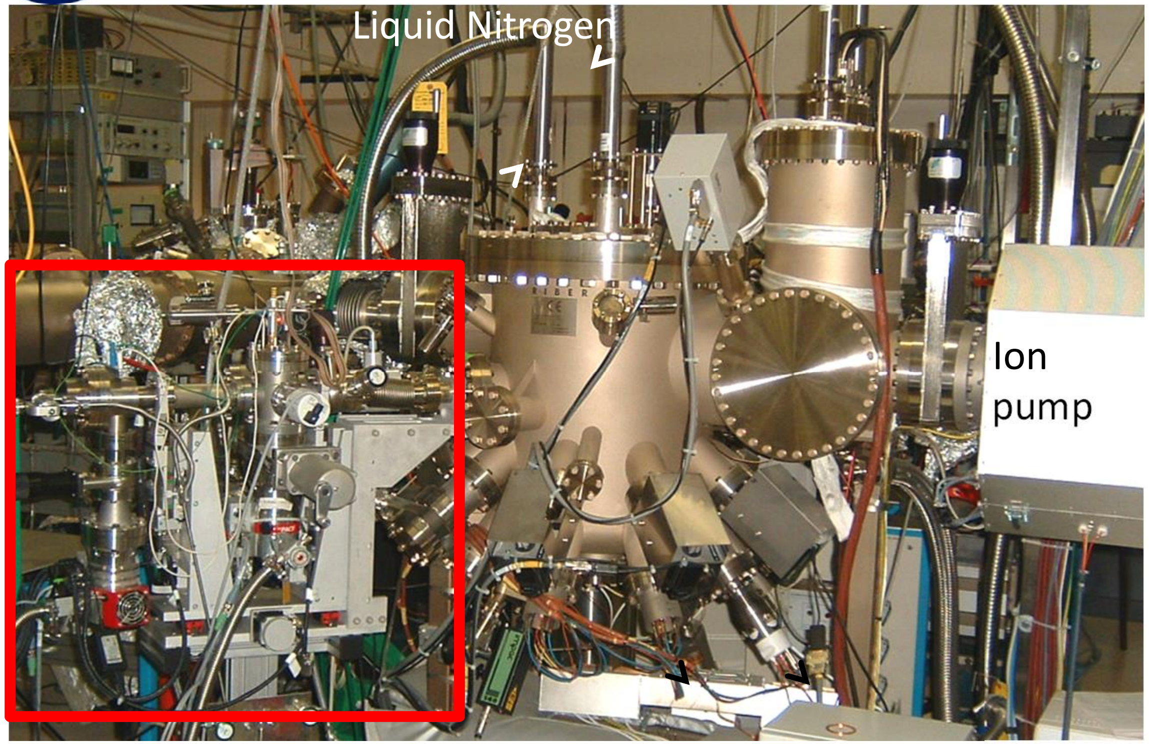

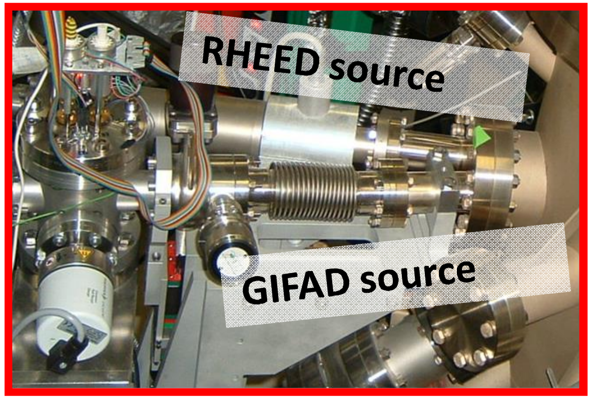

Conventional Riber
Compact 21 MBE machine

Å noble gas ion pump
Å slightly larger in/out flanges for RHEED/GIFAD

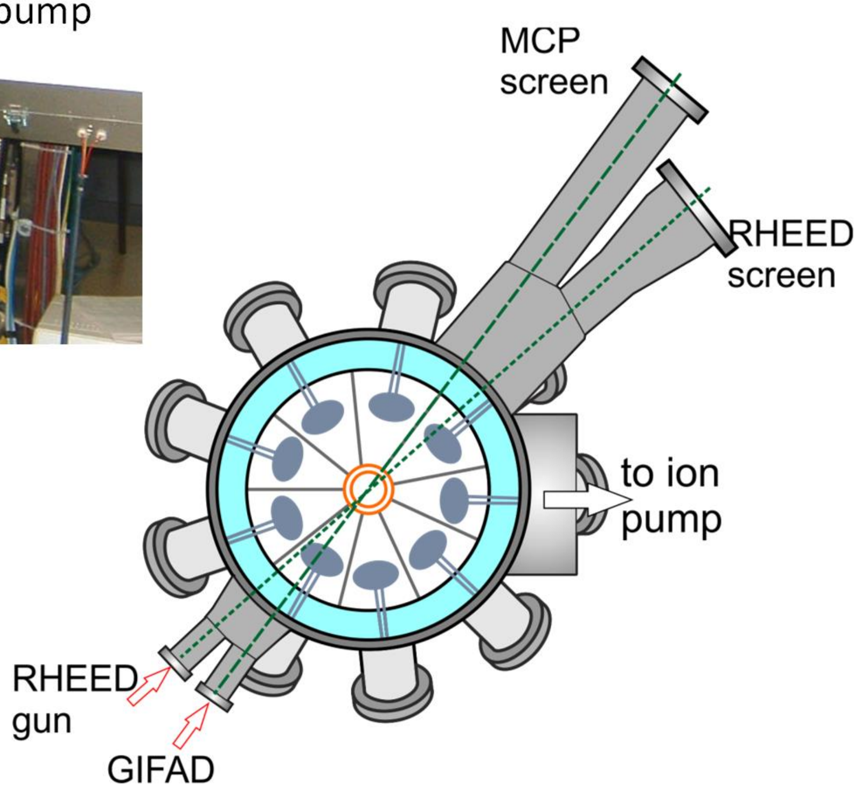

GIFAD on an MBE chamber

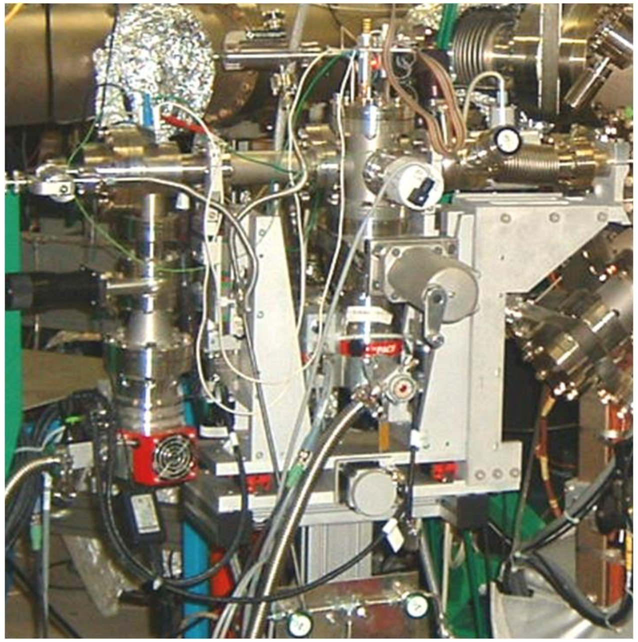

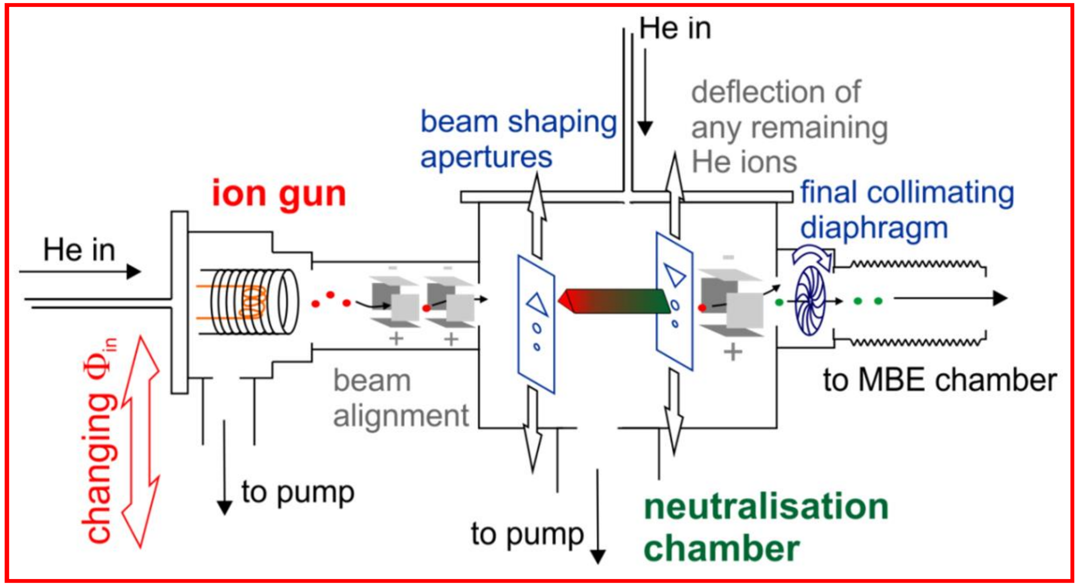

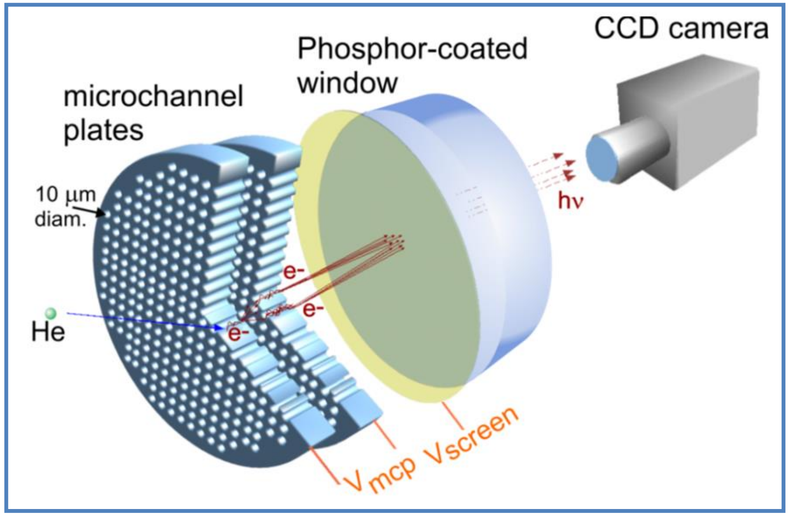

Typical ion gun voltage: 300 eV – 1 keV
He pressure in ion gun: ~ 3×10^{-8} mbar
in neutralisation chamber: ~ 3×10^{-6} mbar
Efficiency of neutralisation approx 10%
Beam diameter after collimation ~ 50 ï 100μm
divergence $\Delta\phi$~ 1 mrad (< 0.03 degrees)
Lateral coherence of beam = $\lambda/\Delta\phi$
Net Helium beam flux into growth chamber:
~ 10^{11} – 10^{12} atoms cm^{-2} s^{-1}
MCP multiplication ~ 10^4

GaAs (100) surface

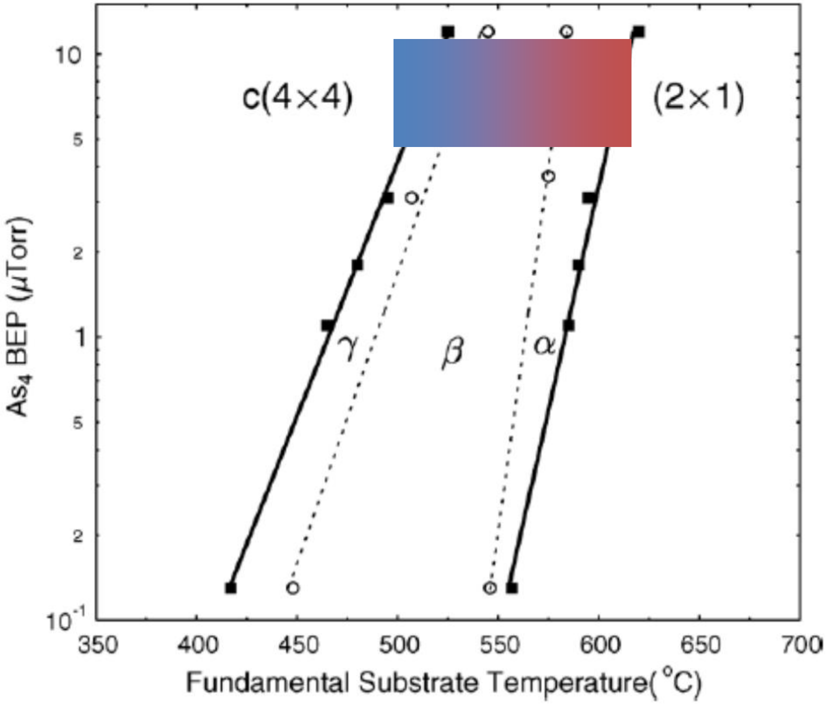

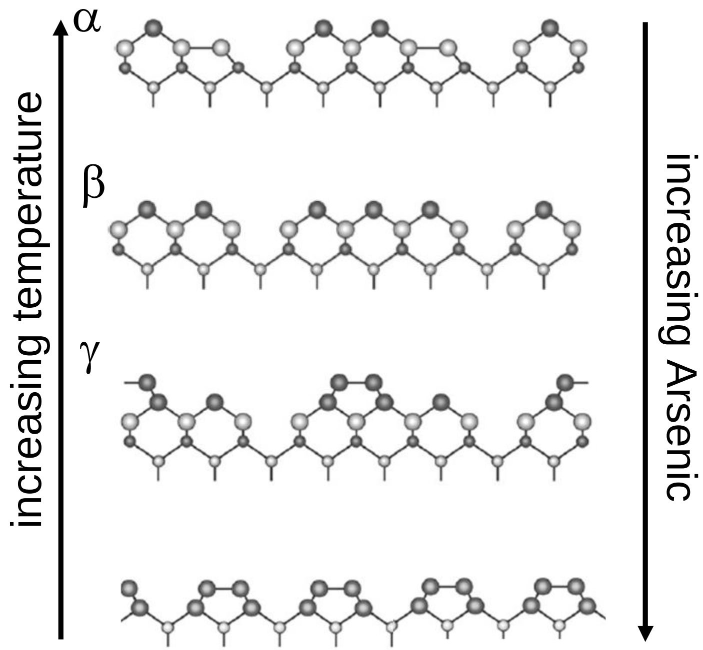

Along [-110], pattern changes from x2 to x4

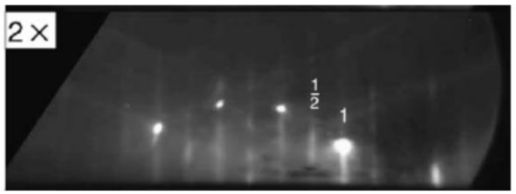

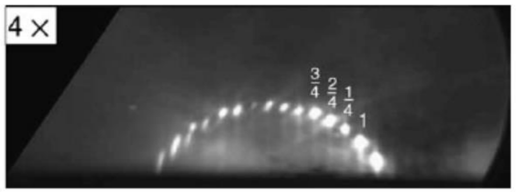

LaBella et al. Surf. Sci. Reports. 60 (2005) 1, Ohtake et al. Surf Sci Reports 63 (2008) 295

Diffraction under « real » conditions

<u>Requirements:</u>

Measurement of surface reconstruction/crystal structure

✓ Possible at substrate temperatures > 600 deg C

Calibration of growth rate

✓ Up to 0.5 ML/s in layer-by-layer growth mode

(future gun developments will allow higher values)

Determination of growth mode

✓ Possible

Assessment of surface quality / terrace length / defect density

Ongoing...

Measurement of surface chemical composition

Future development...

✓ In-situ and non-invasive
✓ Real-time
✓ Quantitative interpretation

Surface reconstruction analysis

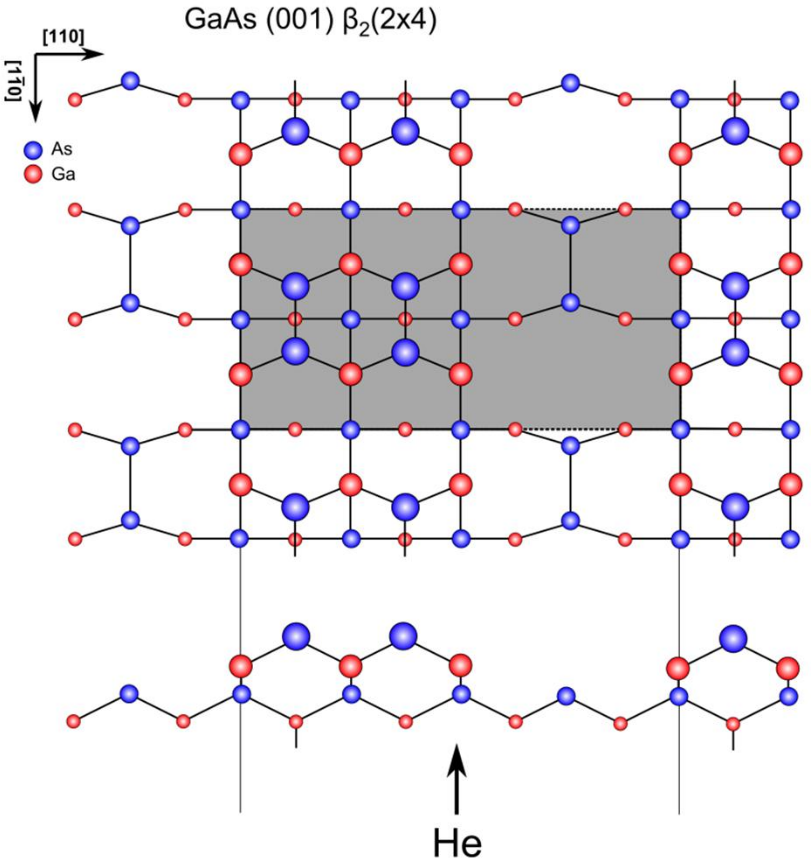

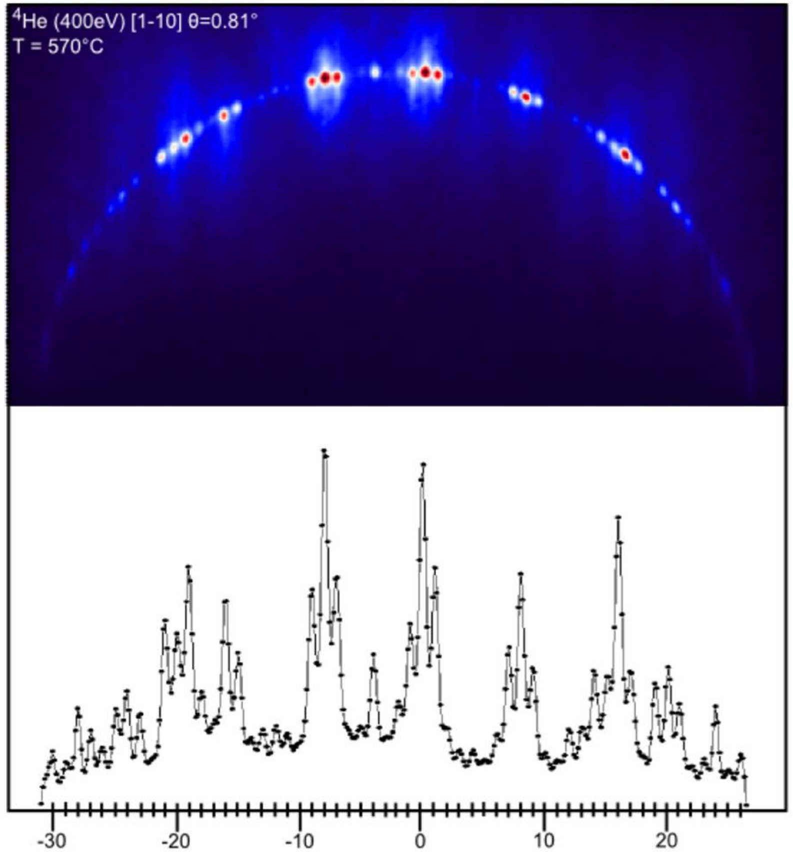

80 diffractions order visible at T_{sub} = 570°C with incident As flux!

GaAs (2×4)β reconstruction

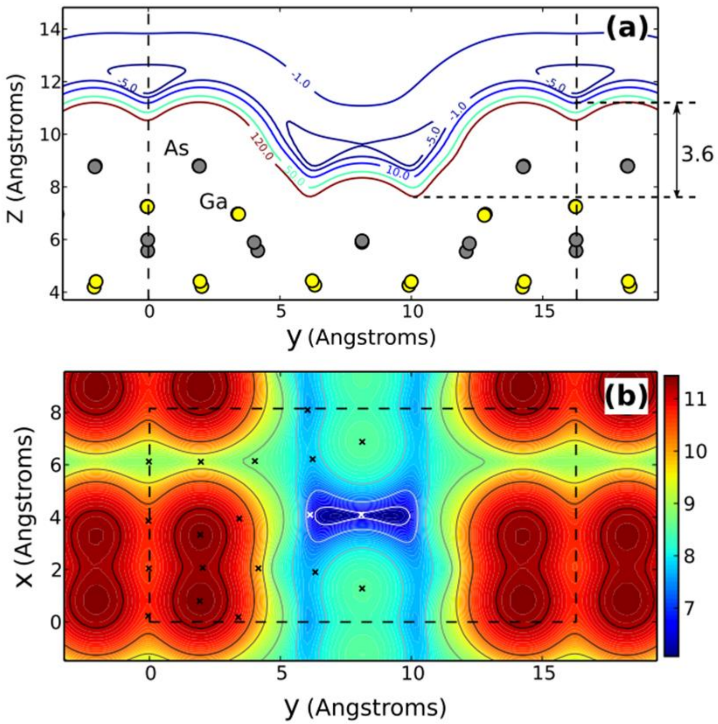

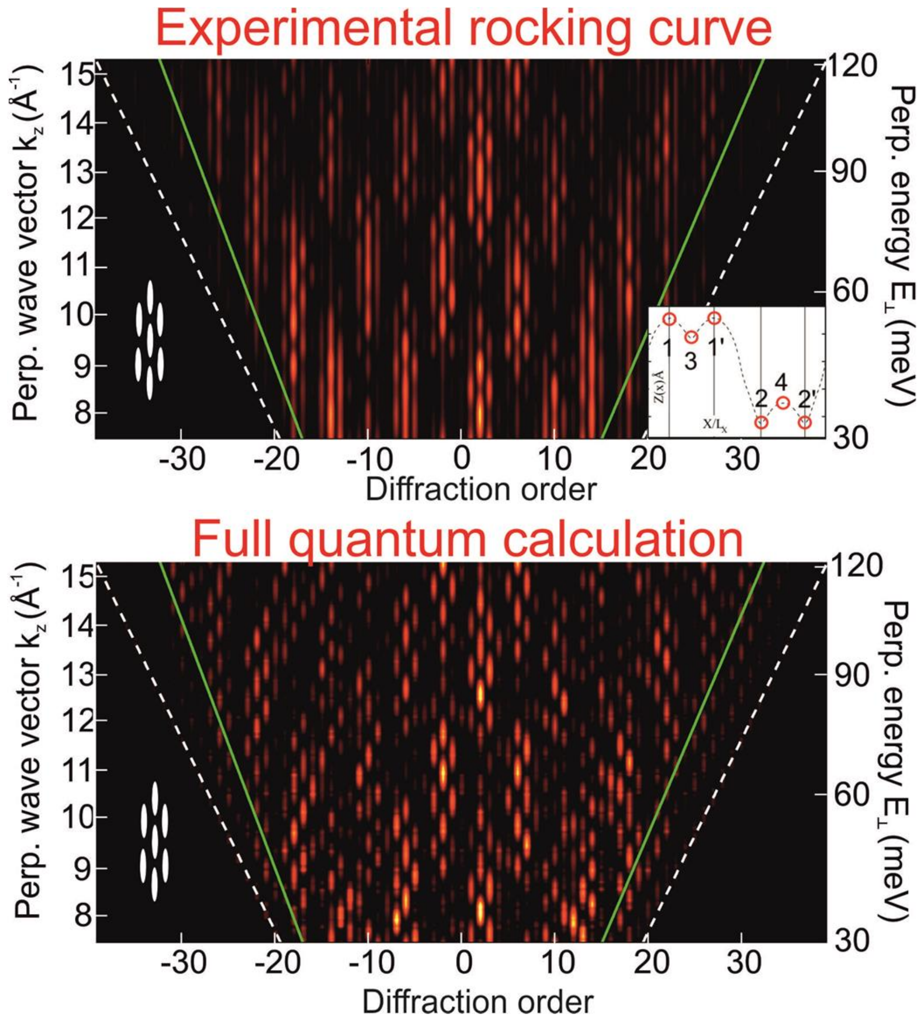

He-GaAs surface potential calculated by DFT
(VASP code with GGA approximation)
Using 13 layers
Van-der-Waals interaction included

Good agreement between theory and expt!

Debiossac et al, PRB 90 155308 (2014)

GaAs (2×4)β reconstruction

Do we need a full quantum wavepacket calculation? Not always!

Semi-classical analysis can simply and quantitatively verify surface reconstructions

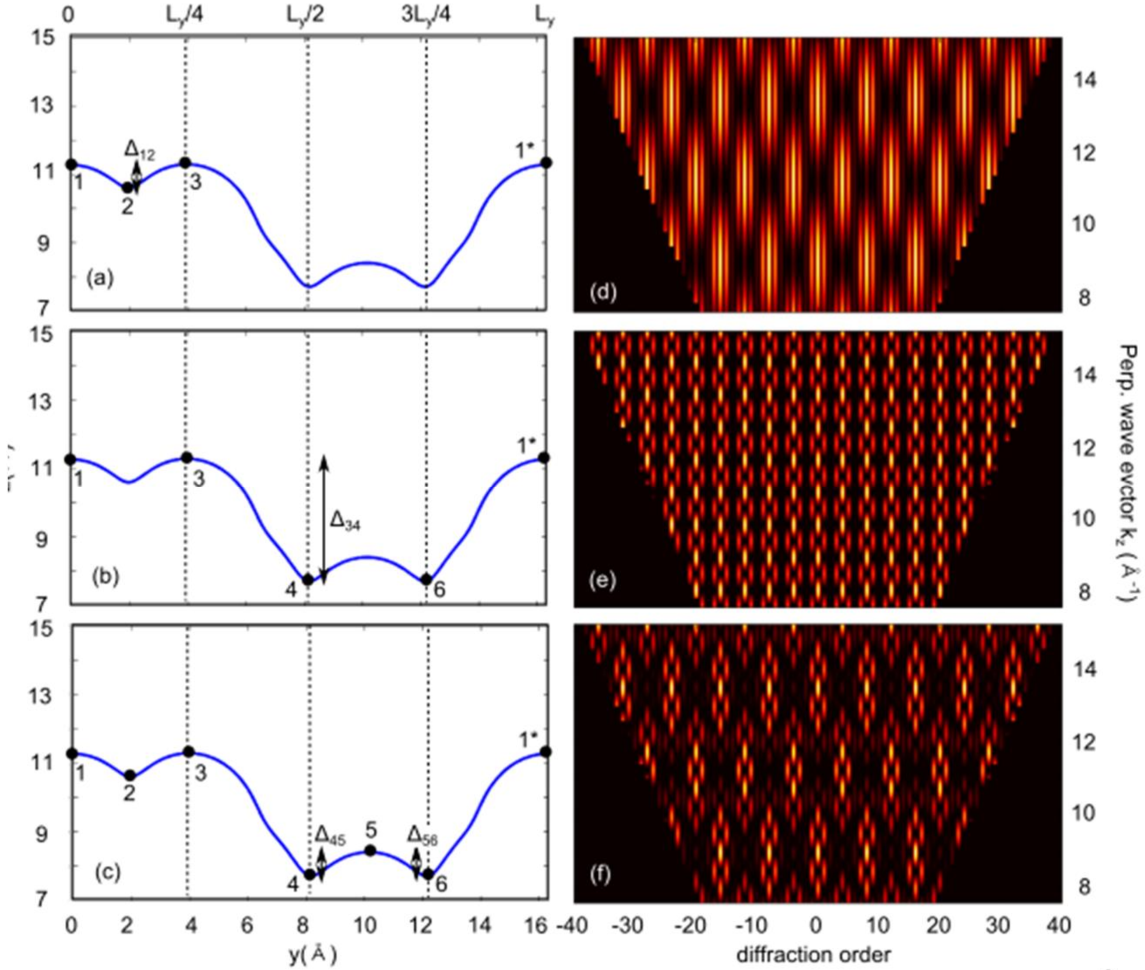

Interference between small valleys and peaks

Interference between large valleys and peaks

Combined interference pattern of He atoms reflected from top and bottom of small and large surface potential valleys

$\Delta_{34} = 3.6\text{Å} \quad \Delta_{12} = \Delta_{45} = \Delta_{56} = \Delta_{34}/5$

Surface reconstruction analysis

Some remaining questions…

Can we use the same potential calculated for the (2x4)β for other reconstructions?

How sensitive is GIFAD to disorder in the reconstruction?

GaAs c(4x4)

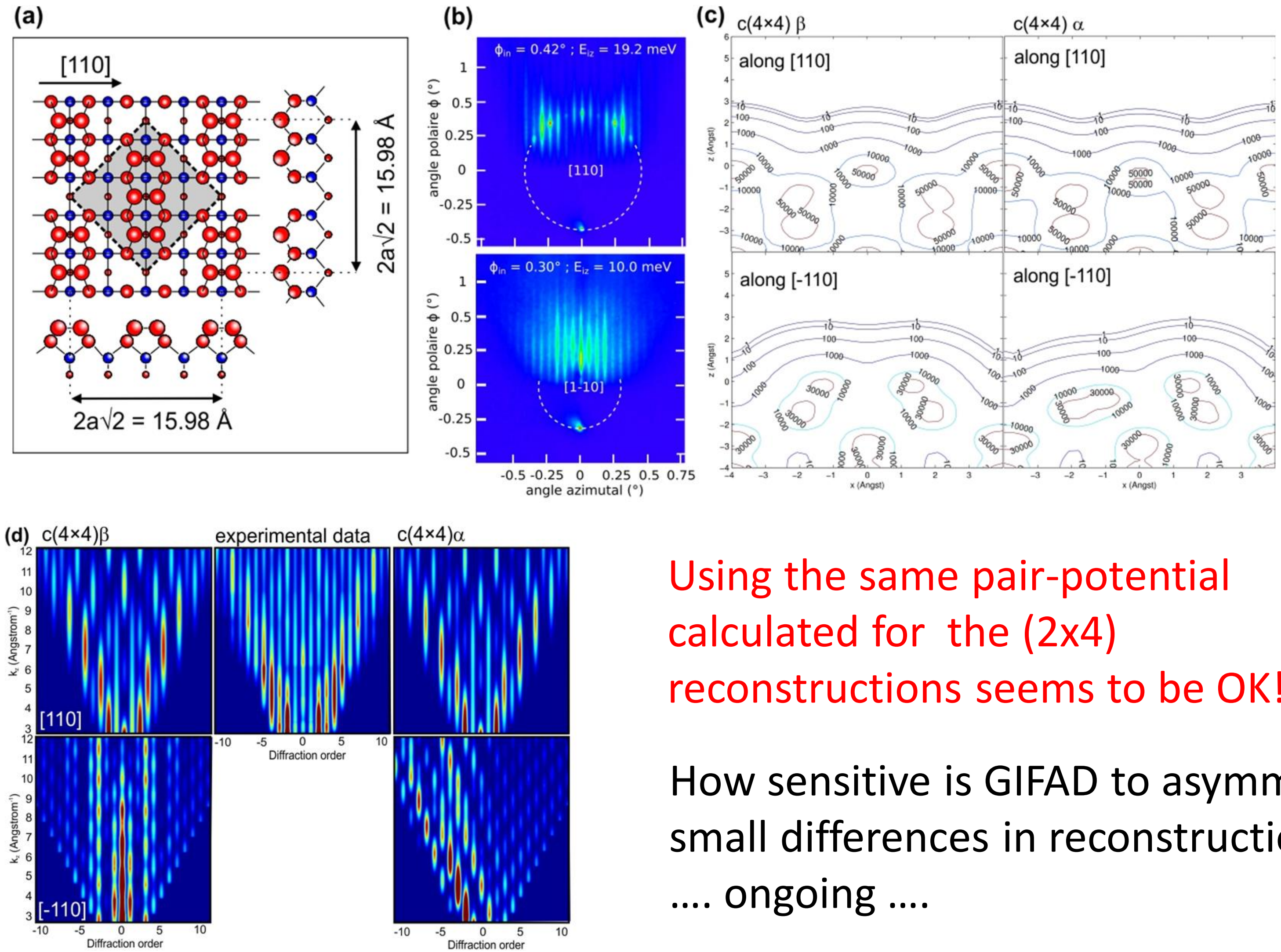

Using the same pair-potential calculated for the (2x4) reconstructions seems to be OK!

How sensitive is GIFAD to asymmetry or small differences in reconstructions?

…. ongoing ….

Sensitivity to disorder...

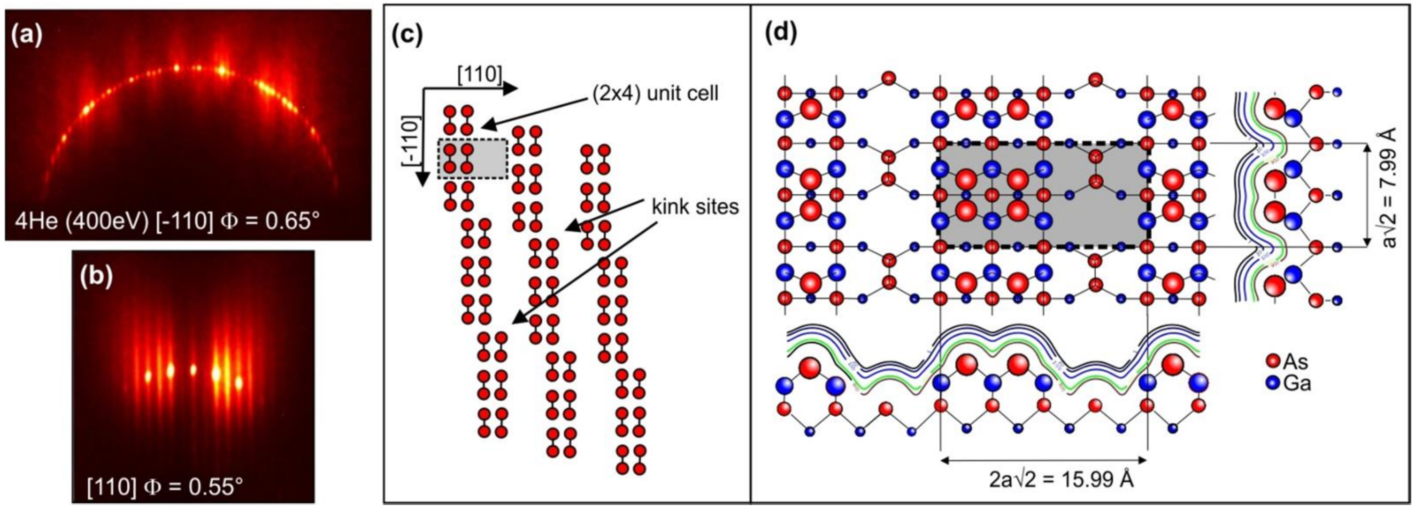

Missing “elastic” diffraction orders along [110] direction

Is this related to disorder in surface reconstruction?

Real-time monitoring

c(4×4) → (2×4) transition

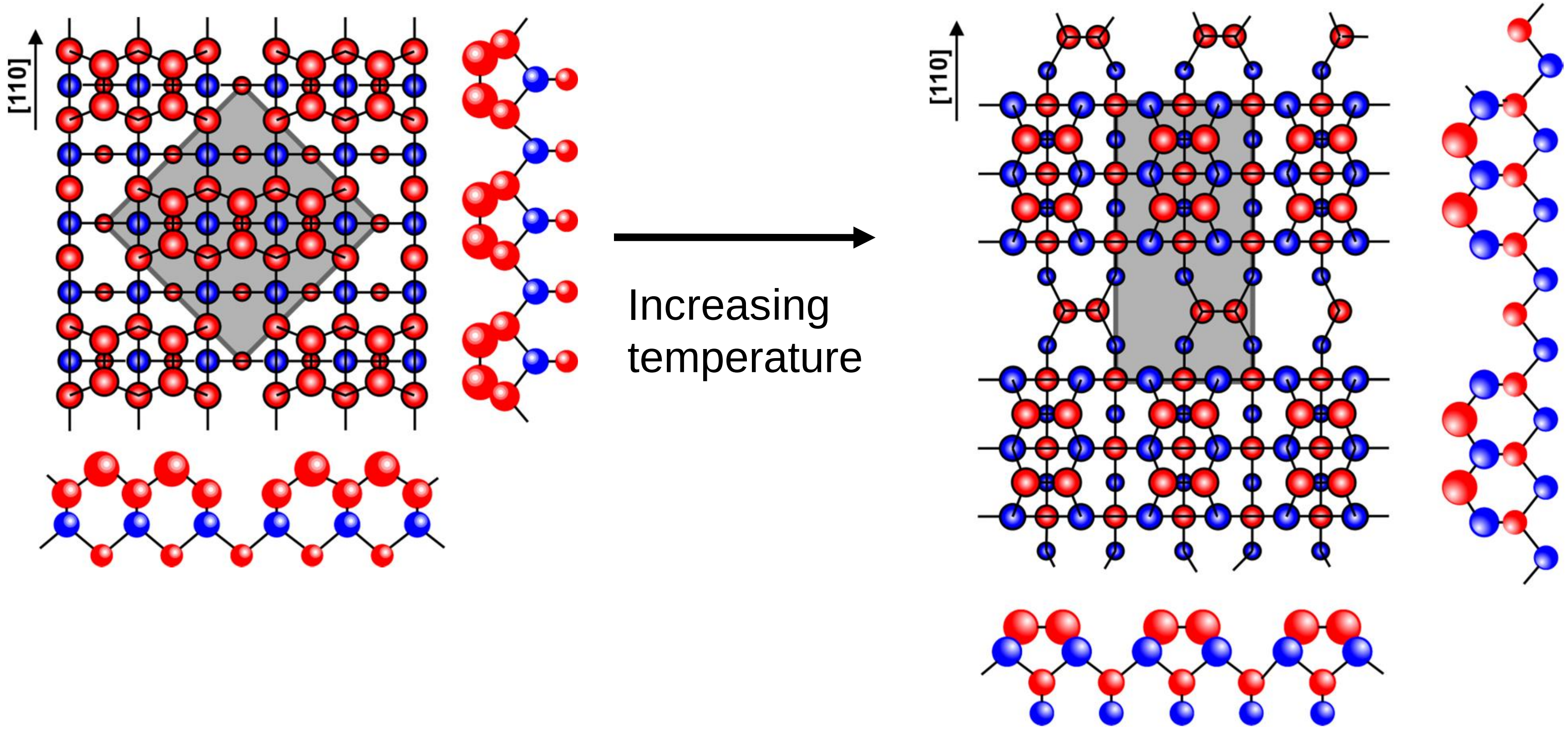

Å As dimers dissociate, exposing Ga atoms

Å Ga atoms migrate, to form small nuclei of (2x4) phase on top of the c(4x4)

Shiraishi et al, Surface Science (1999) 433-435 382

c(4×4) → (2×4) transition

Can we use the change in diffraction pattern to work out *how* a reconstruction transition is occuring?

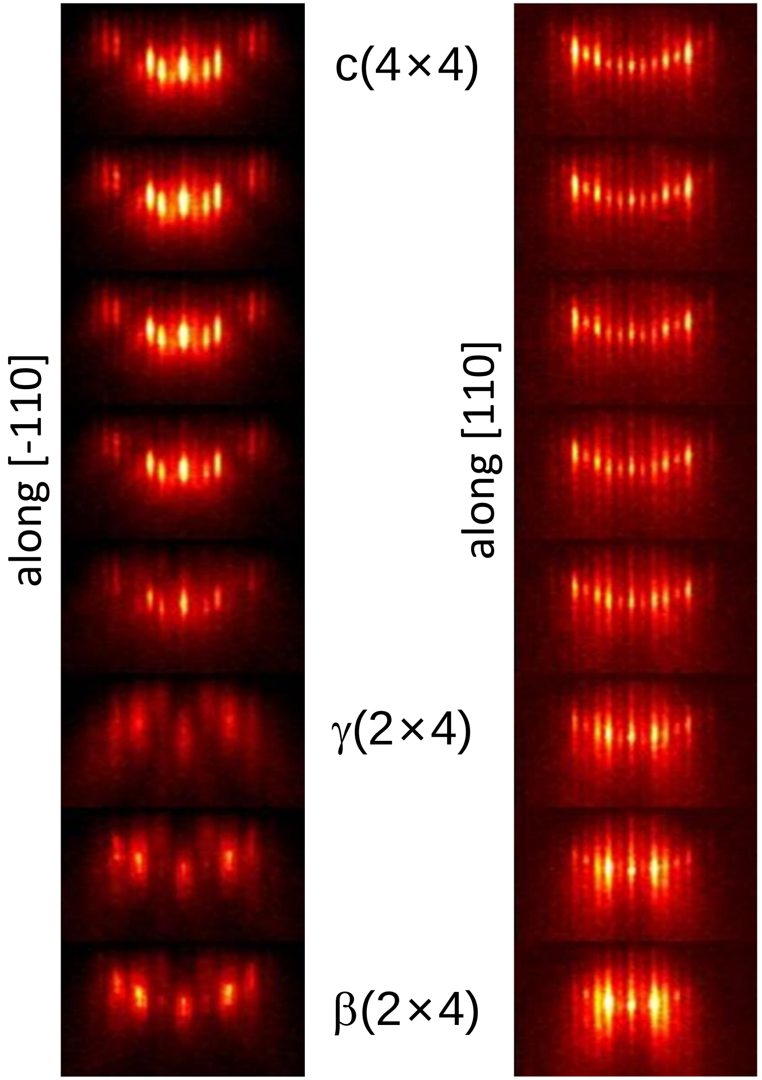

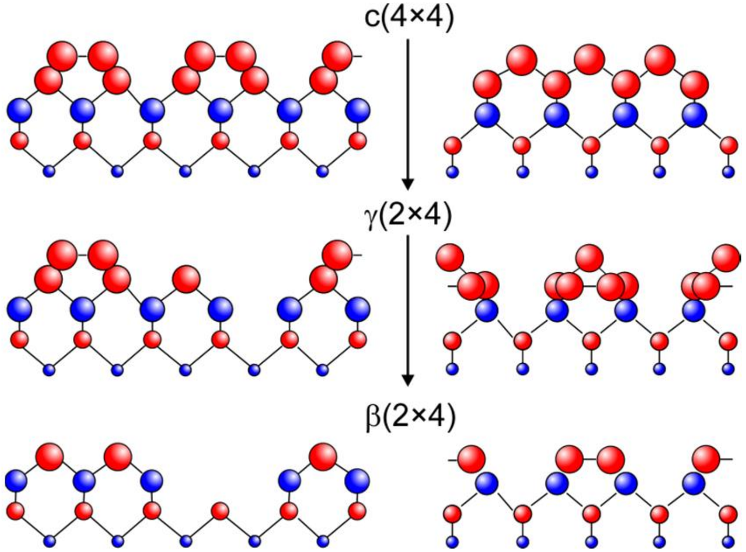

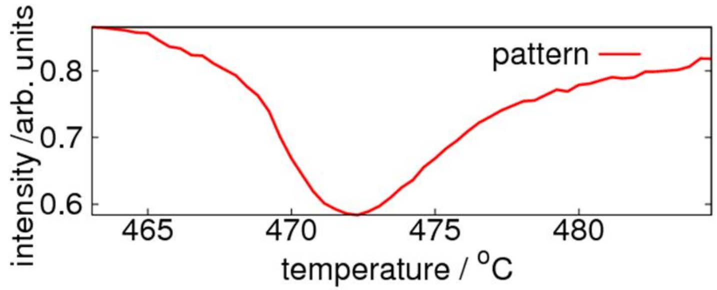

Loss in scattered intensity at phase transition, more marked along [-110] ➔ small nuclei of new phase forming oriented along [110] ?

Growth rate oscillations

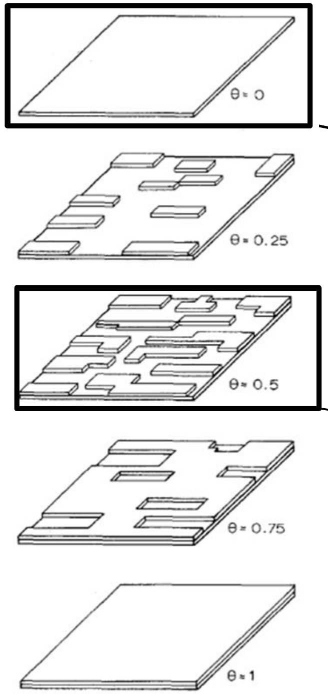

θ is fractional layer coverage

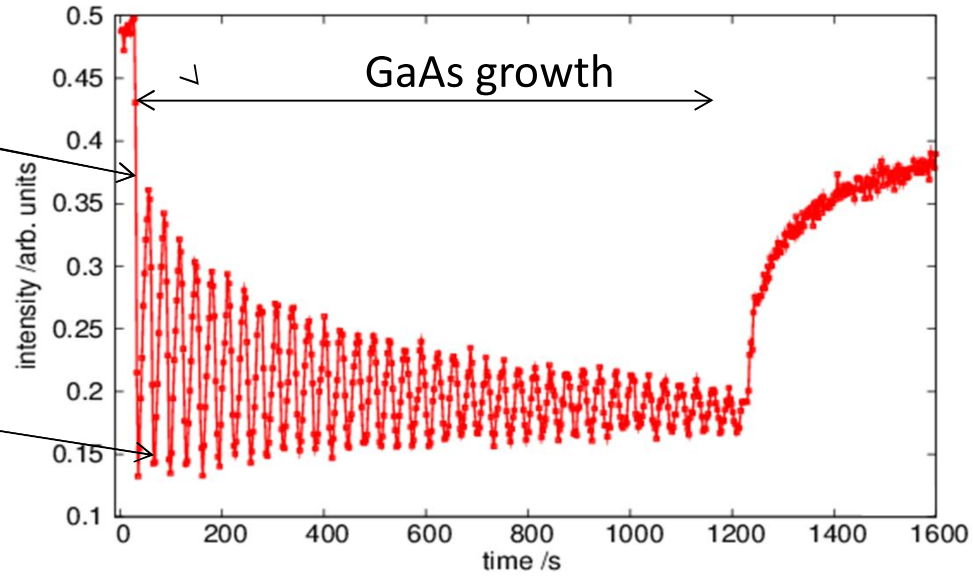

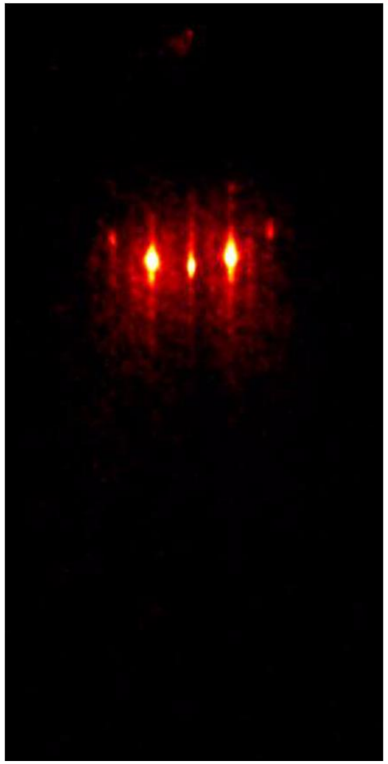

Å All orders oscillate in phase

Video at: http://www.insp.jussieu.fr/IMG/avi/GIFAD.avi

- ✓ Calibration of growth rate
- ✓ Determination of growth mode

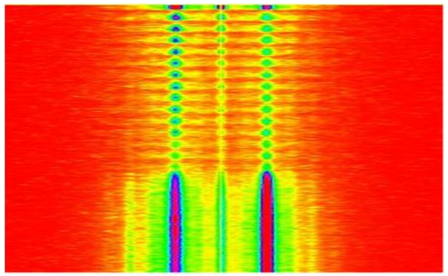

Neave et al. Appl. Phys. A 31 (1983) 1

Growth rate oscillations

RHEED oscillations –
depend on diffraction order
and incidence angle
➔ Oscillation magnitude not simply linked to step density

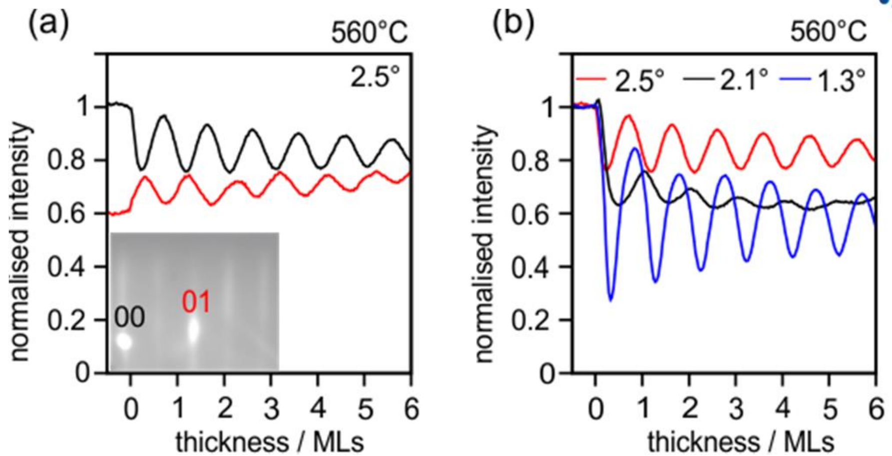

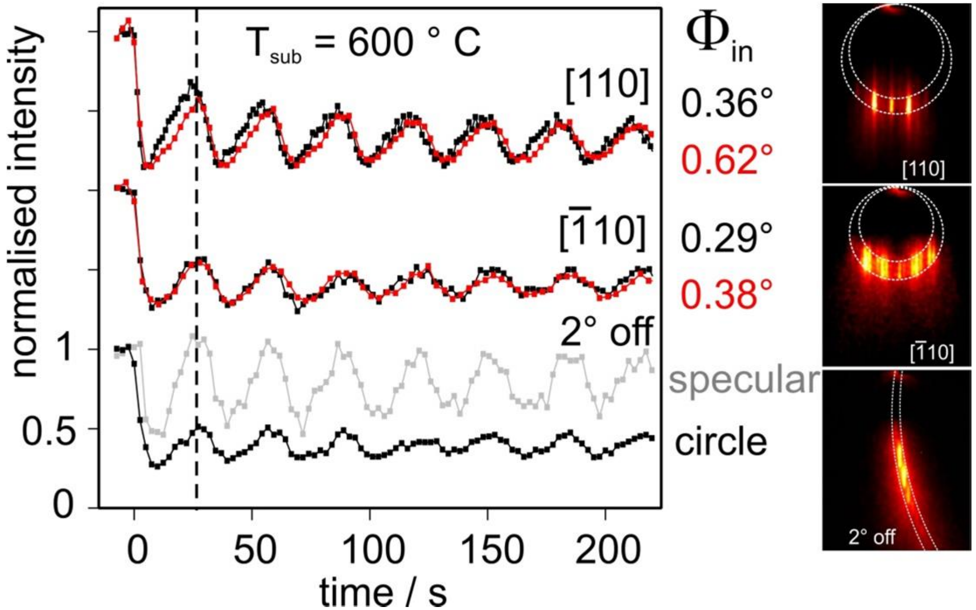

GIFAD is "simpler" than RHEED

No phase shift with incidence angle!

Higher amplitude oscillations along [110] than [-110]

➔ higher step density along [110]

Oscillations also visible along « random » direction

GIFAD intensity directly related to surface roughness

Growth rate oscillations

On the Laue circle, all the diffraction orders oscillate in phase

The **superspecular** scattered intensity oscillates in advance of the **specular** intensity

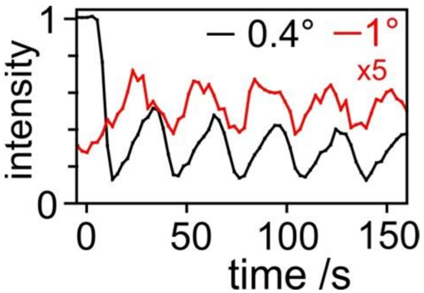

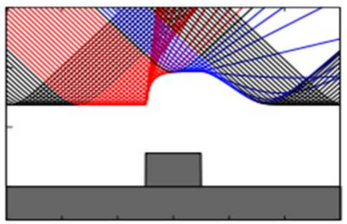

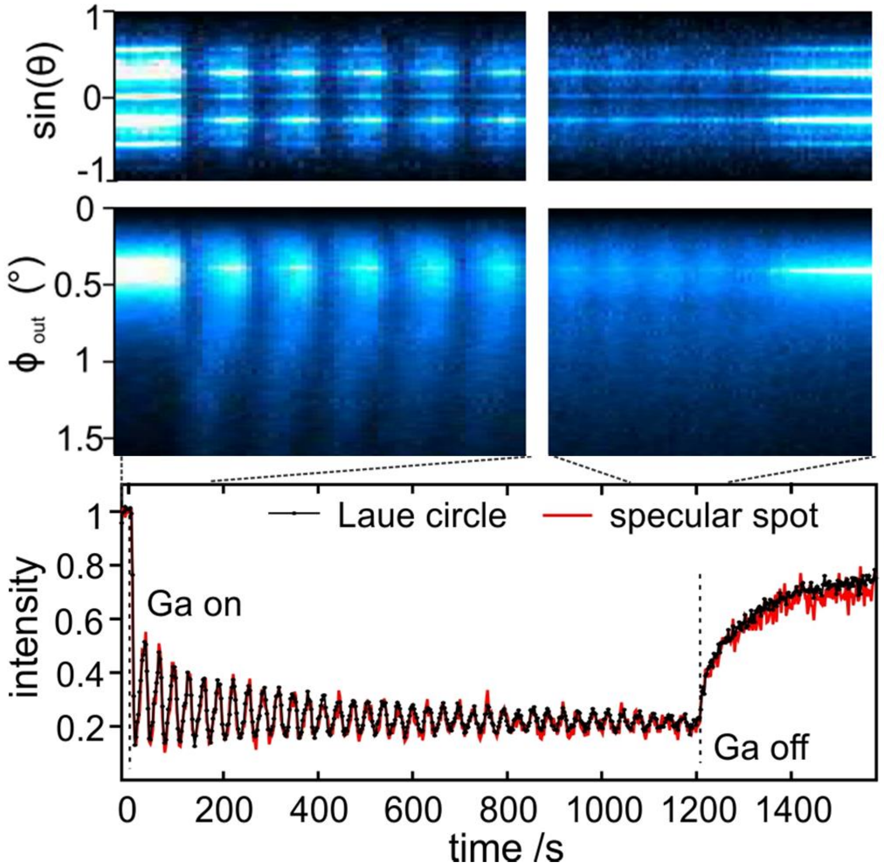

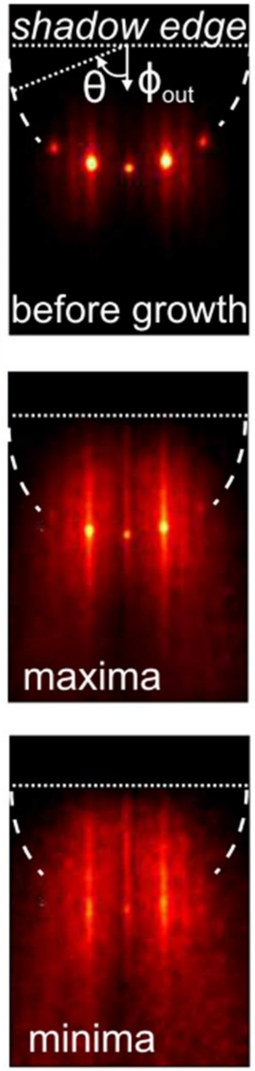

Diffraction still visible at minima : terraces wider than the beam lateral coherence length (~ 30 Å)

Atkinson et al, APL 105 021602 (2014),

Growth rate oscillations

Small change in relative intensity of diffraction orders
➔ change in corrugation.
Possibility to determine attachment sites during growth?

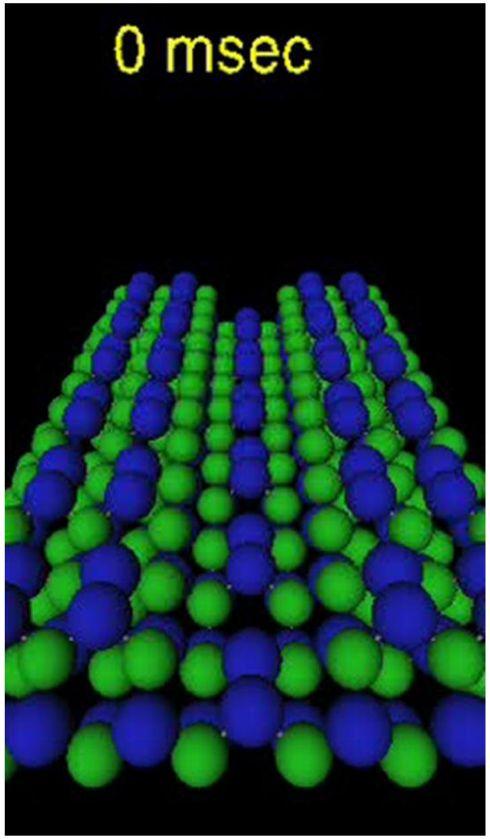

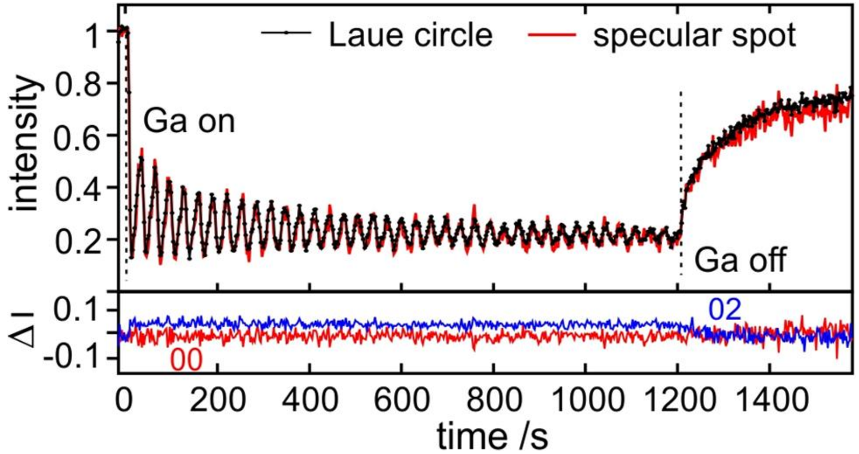

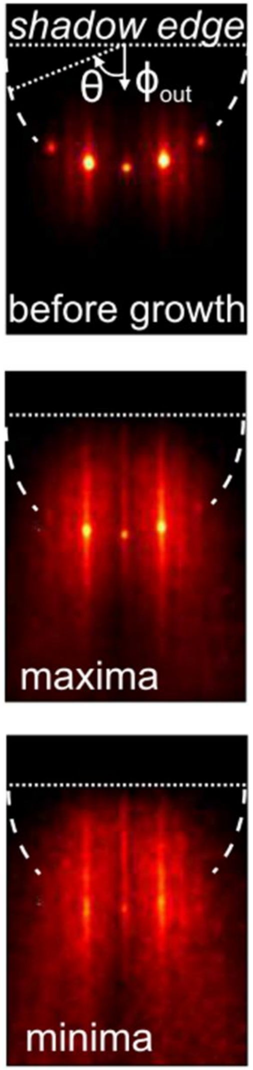

Monte Carlo simulations indicate that attachment occurs in trenches first

Video at:

http://ftp.aip.org/epaps/phys_rev_lett/E-PRLTAO-87-031152/

Kratzer and Scheffler, PRL (2002) 88 036102 ***Atkinson et al, APL 105 021602 (2014),***

Growth rate oscillations

Disclaimer:
Diffraction conditions not needed for simply monitoring growth rate

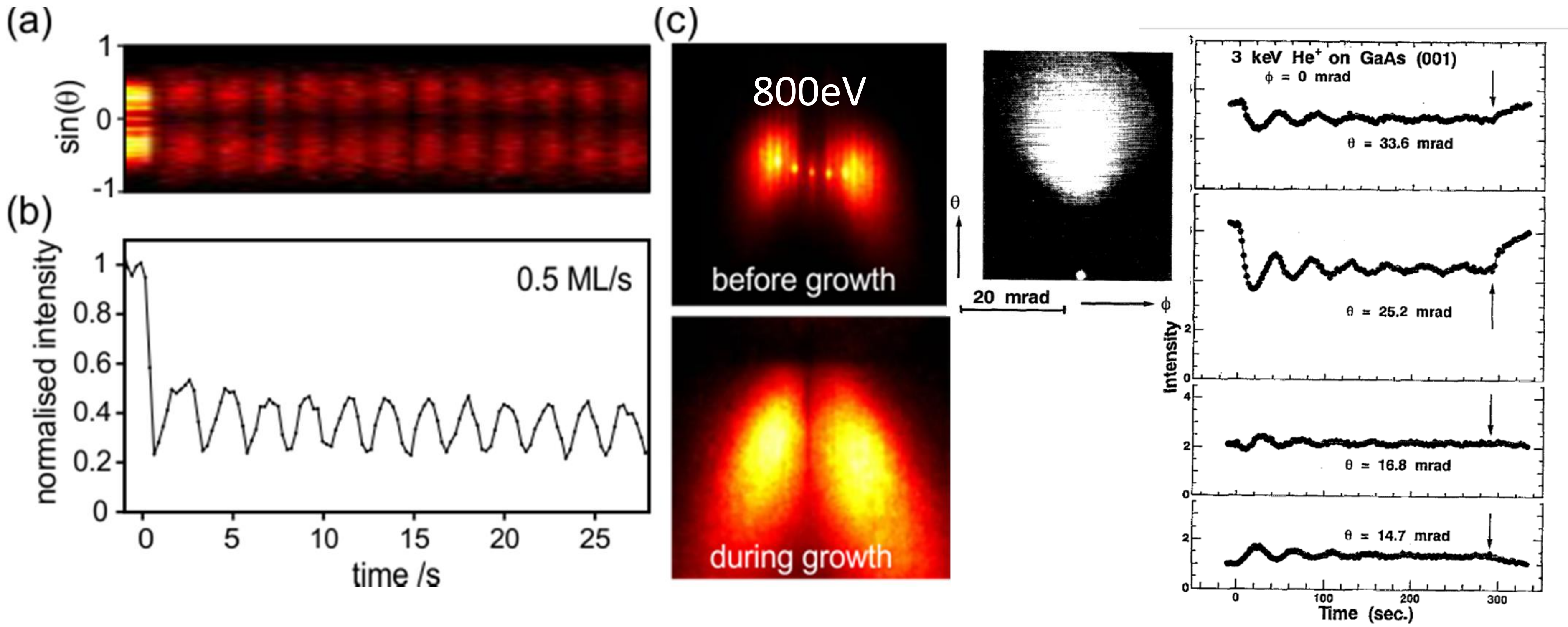

Atkinson et al, APL 105 021602 (2014), Fujii et al, APL 63 2070 (1993)

Growth rate oscillations

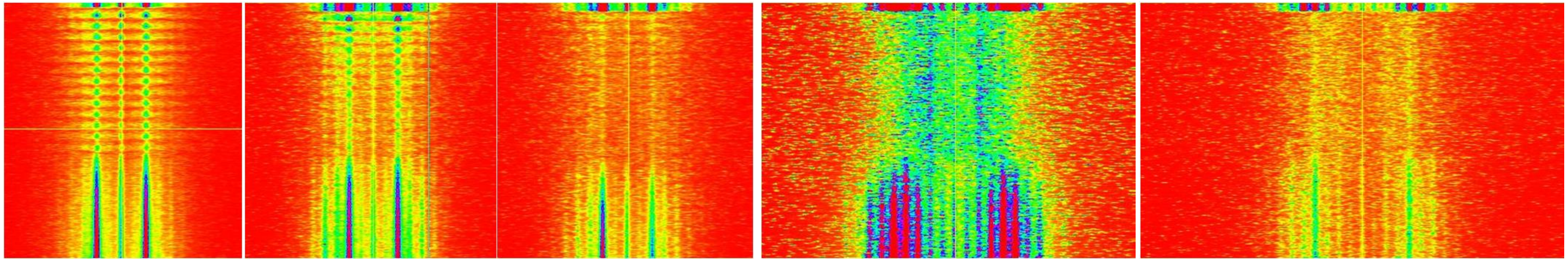

580°C 540°C 505°C 465°C 425°C

Can use GIFAD to assess growth dynamics

➔ Decreasing growth temperature

= increased roughening,

= slower surface recovery

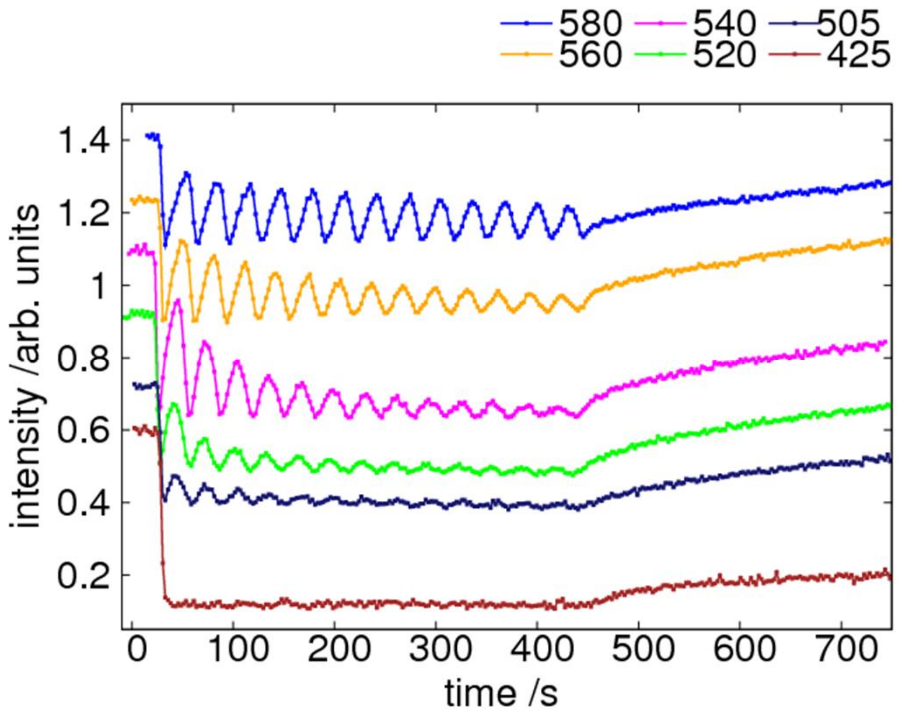

Effect of temperature & reconstruction

GIFAD

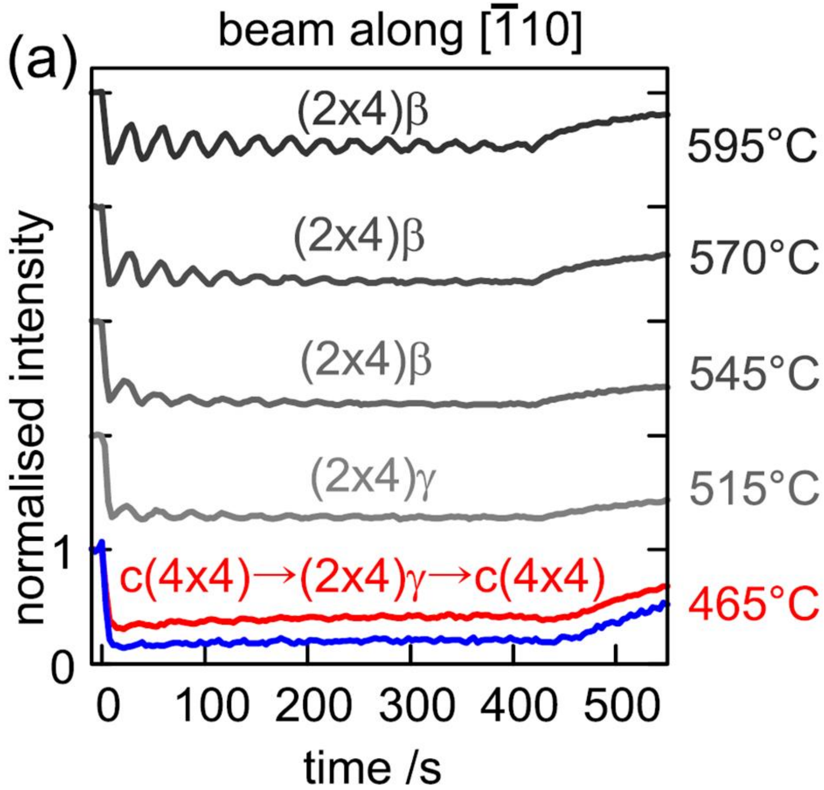

RHEED

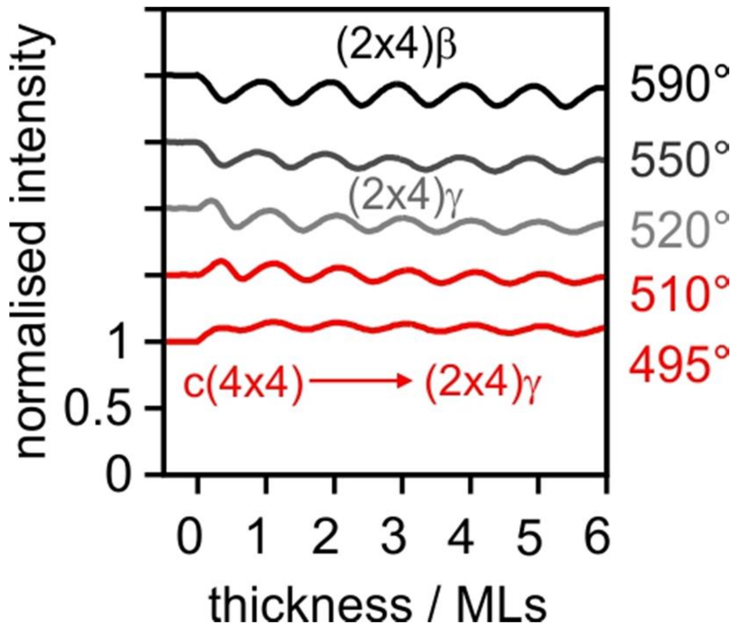

At 465 °C : Difference between relative intensity of specular spot and scattered intensity on Laue circle

Change in initial transient in RHEED when surface reconstruction changes

➔ RHEED not a direct measure of surface roughness

Atkinson et al, APL 105 021602 (2014),

Effect of temperature & reconstruction

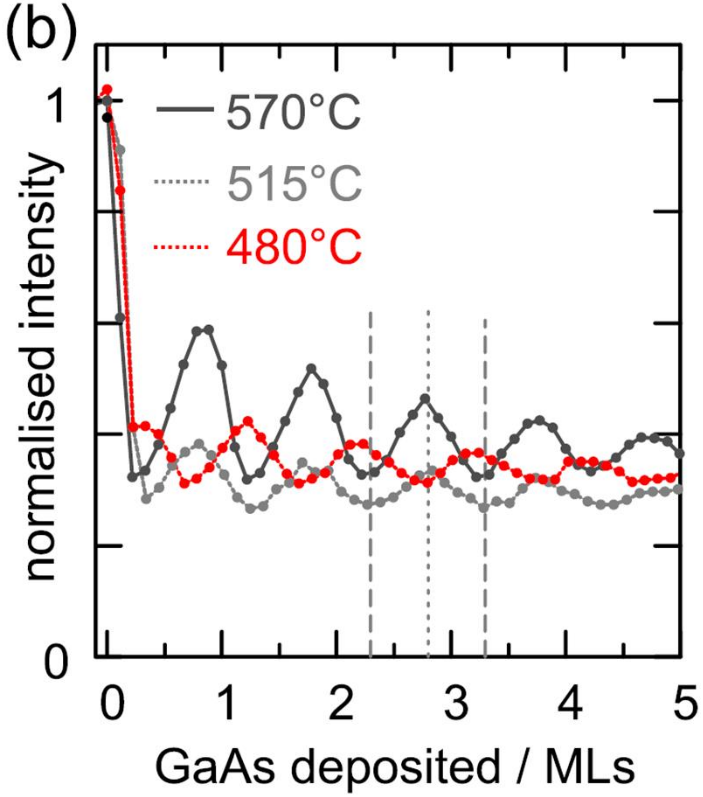

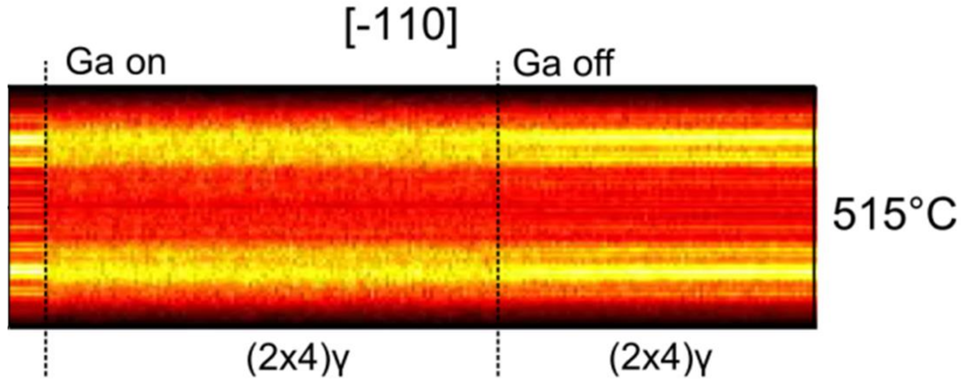

Intensity along the Laue circle normalised to the integrated intensity vs. time

No change in the surface reconstruction during growth at 515°C

Atkinson et al, APL 105 021602 (2014),

Effect of temperature & reconstruction

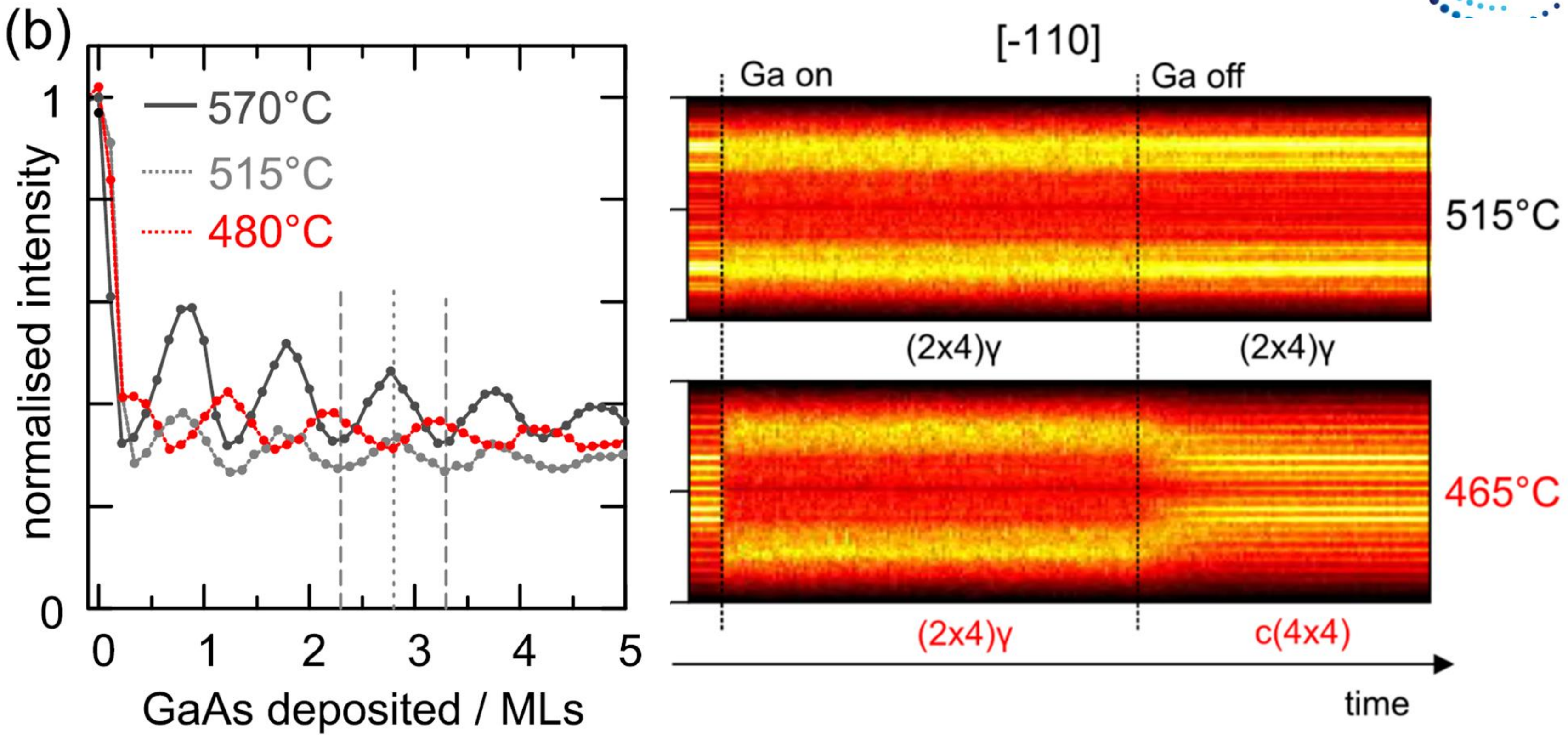

Change in surface reconstruction at 465°C = delay in onset of growth oscillations

Å At 465 °C : Surface reconstruction transition during growth, consumes 0,4 ML Ga

Å In close agreement with theoretical calculations of the difference in excess As on the surface of the c(4×4) and (2×4)β reconstructions, [c.f. Ishizaki, Appl. Surf. Sci (2005)]

Atkinson et al, APL 105 021602 (2014)

Sensitivity to surface « quality »

Sensitivity to surface « quality »

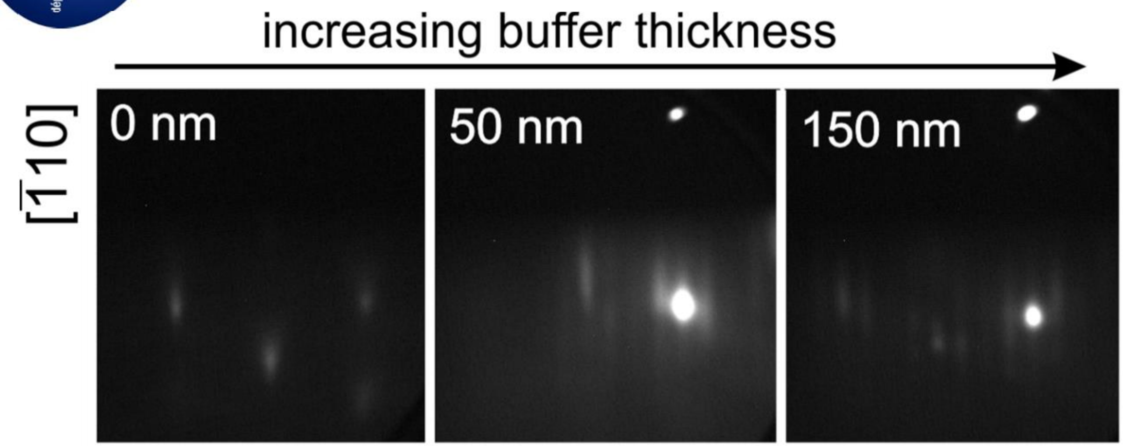

Increasing buffer thickness,
➔ Flatter GaAs surface
➔ RHEED spots get sharper
➔ GIFAD diffraction pattern starts to become evident

After deoxidation: ~ $10^9 - 10^{10}$ cm^{-2}, 2 – 10 nm pits
➔ spotty RHEED
➔ no GIFAD

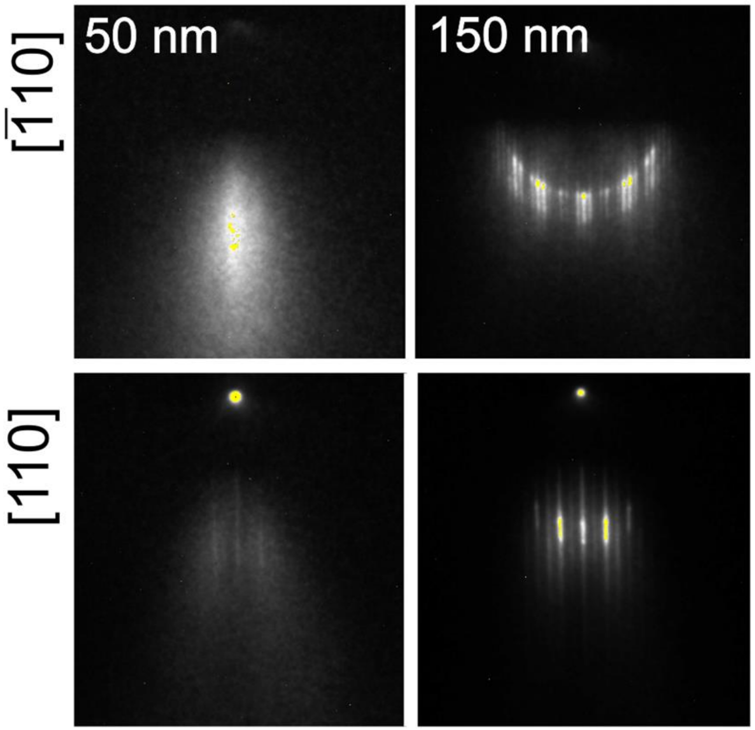

annealing at high temp

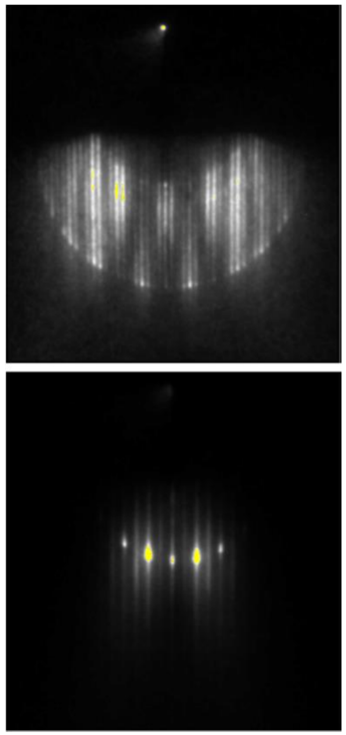

Sensitivity to surface « quality »

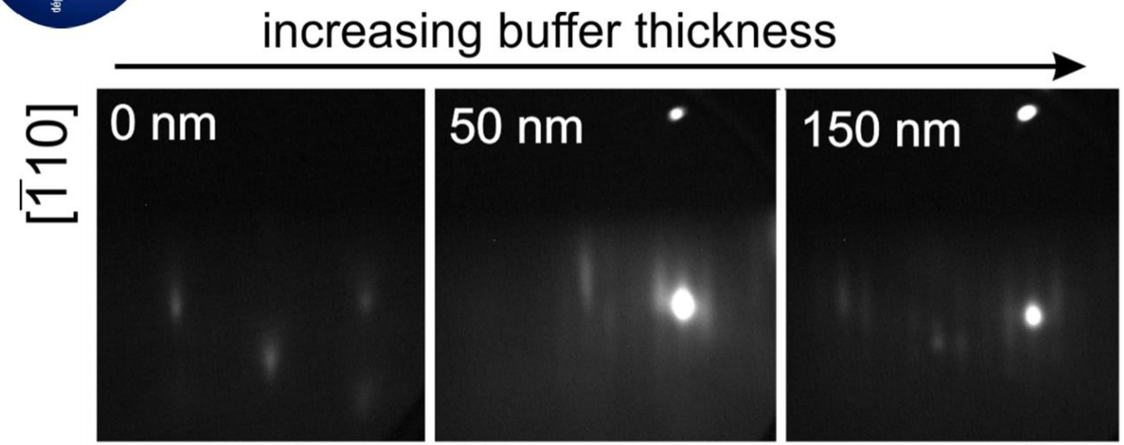

Increasing buffer thickness,
- ➔ Flatter GaAs surface
- ➔ RHEED spots get sharper
- ➔ GIFAD diffraction pattern starts to become evident

After deoxidation:
~ $10^9 - 10^{10}$ cm^{-2}, 2 – 10 nm pits
- ➔ spotty RHEED
- ➔ no GIFAD

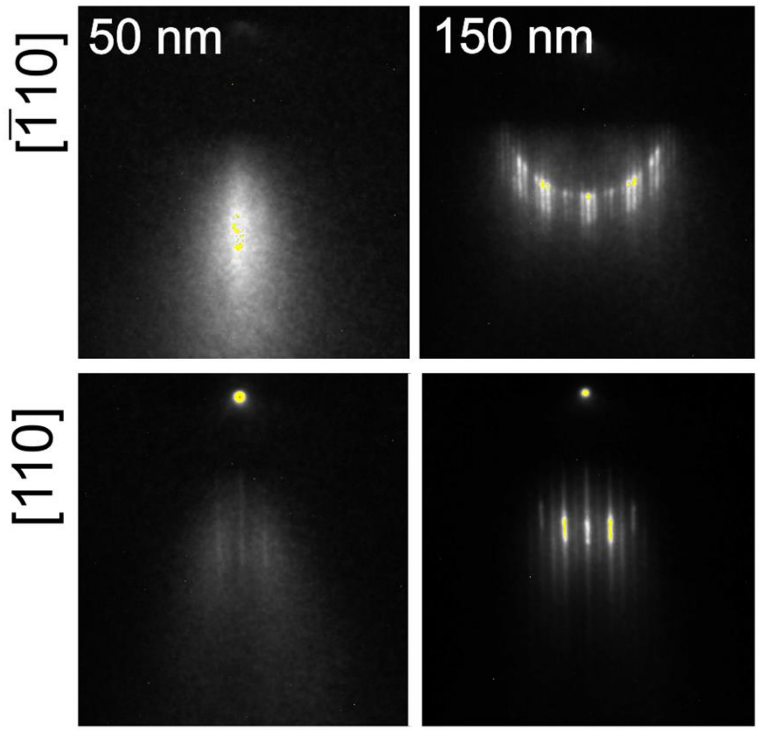

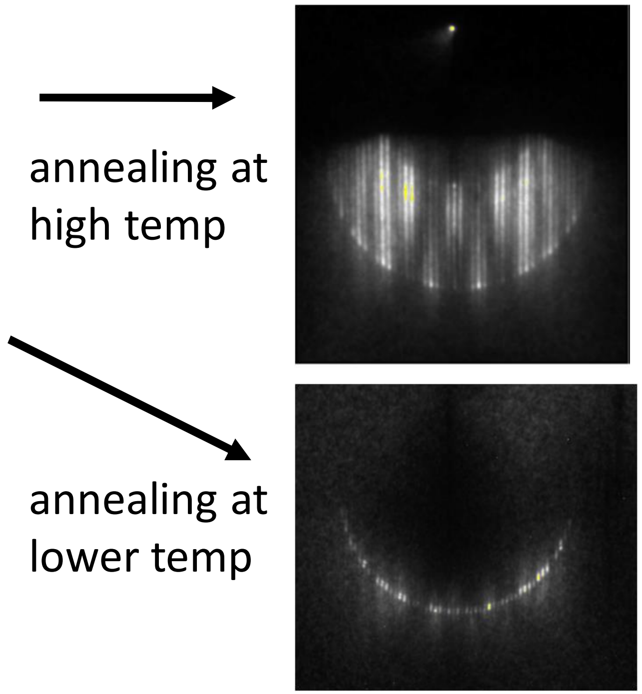

Limitations : 2D-3D transition

Example: InAs growth on GaAs

RHEED : clear transition from
2D to 3D growth
(streaky -> spotty)

GIFAD: diffraction pattern lost once
3D growth is established
(large angle scattering)

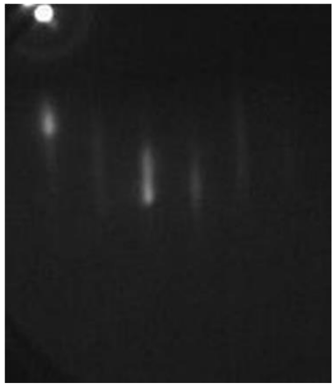

2D growth

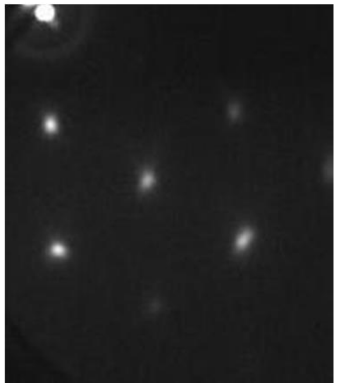

3D growth

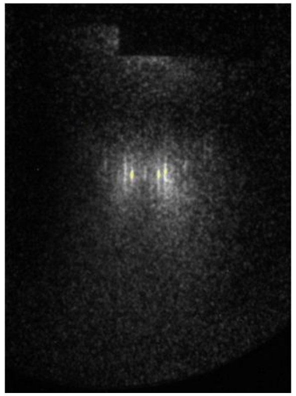

2D growth

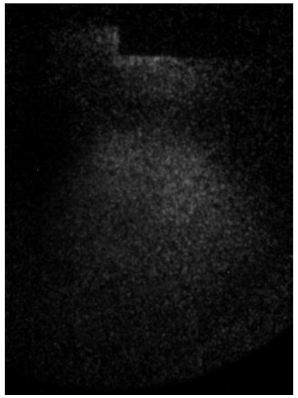

disordered

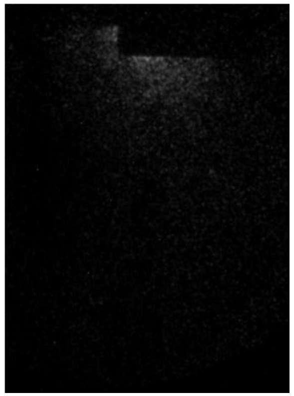

3D growth

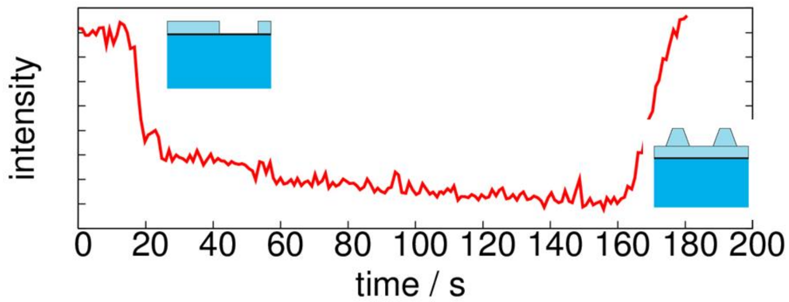

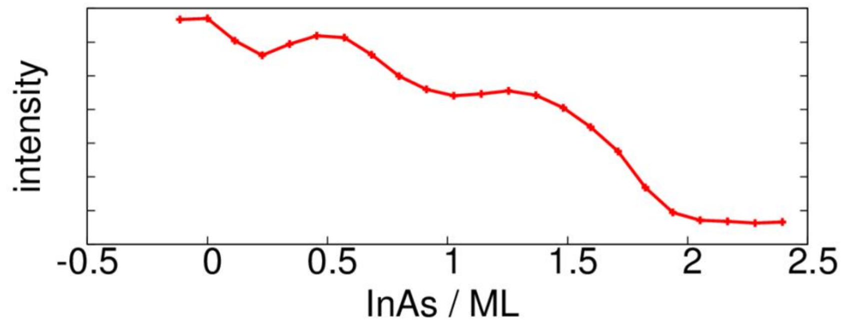

Measuring mosaicity

GIFAD – large area, surface sensitive, precise method to measure mosaicity

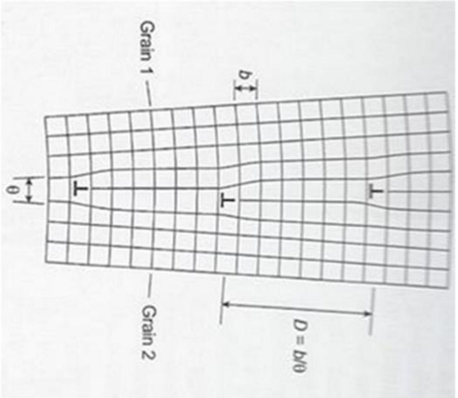

Periodic pattern of dislocations
➔ low-angle grain boundary
➔ tilts (out of plane) or twists (in plane) of crystal planes
➔ separate regions (grains) with perfect crystal structure

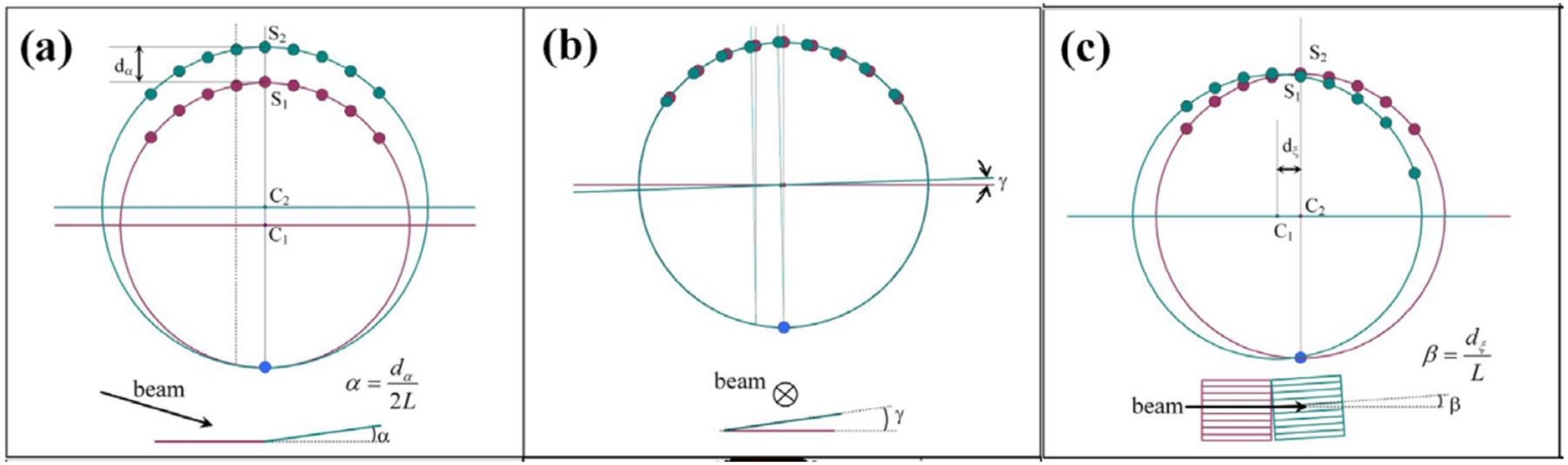

Tilt perpendicular to beam

Tilt parallel to beam

Twis t

Lalmi et al, J. Phys. Condens. Matter, 24, 442002 (2012)

Measuring mosaicity

Example: NaCl (001) and KBr (001), 450eV He beam

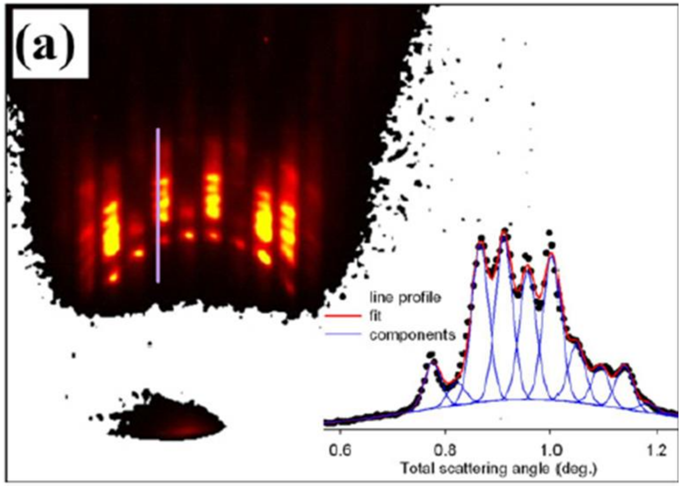

Each spot corresponds to diffraction from a tilted domain

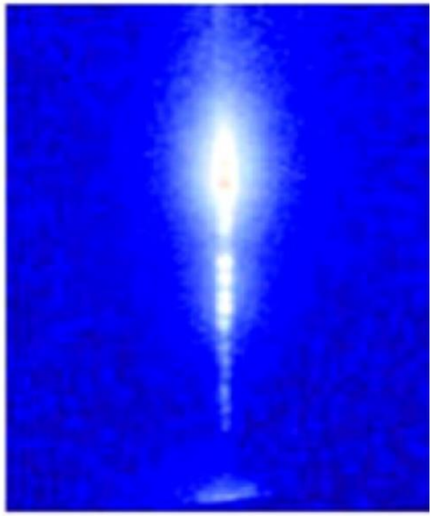

Diffraction not required… "Random" direction as sensitive to tilted domains

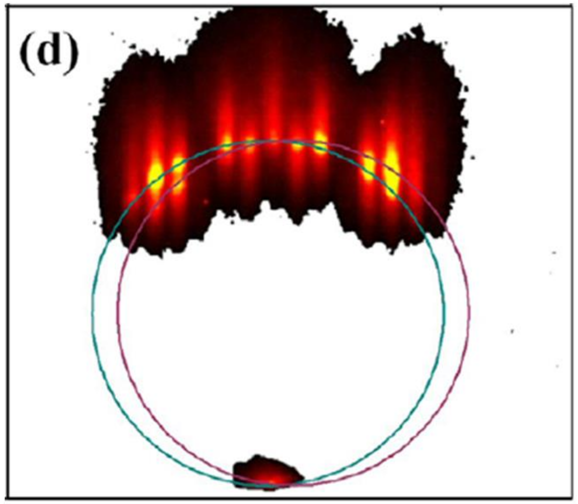

Diffraction from twisted domains

Tilt angles as small as 0.01° can be resolved

Note: domain size can be inferred by looking at the Bragg spot intensities when scanning the beam acoss the sample (in this case a few 100 microns)

Lalmi et al, J. Phys. Condens. Matter, 24, 442002 (2012)

Graphene

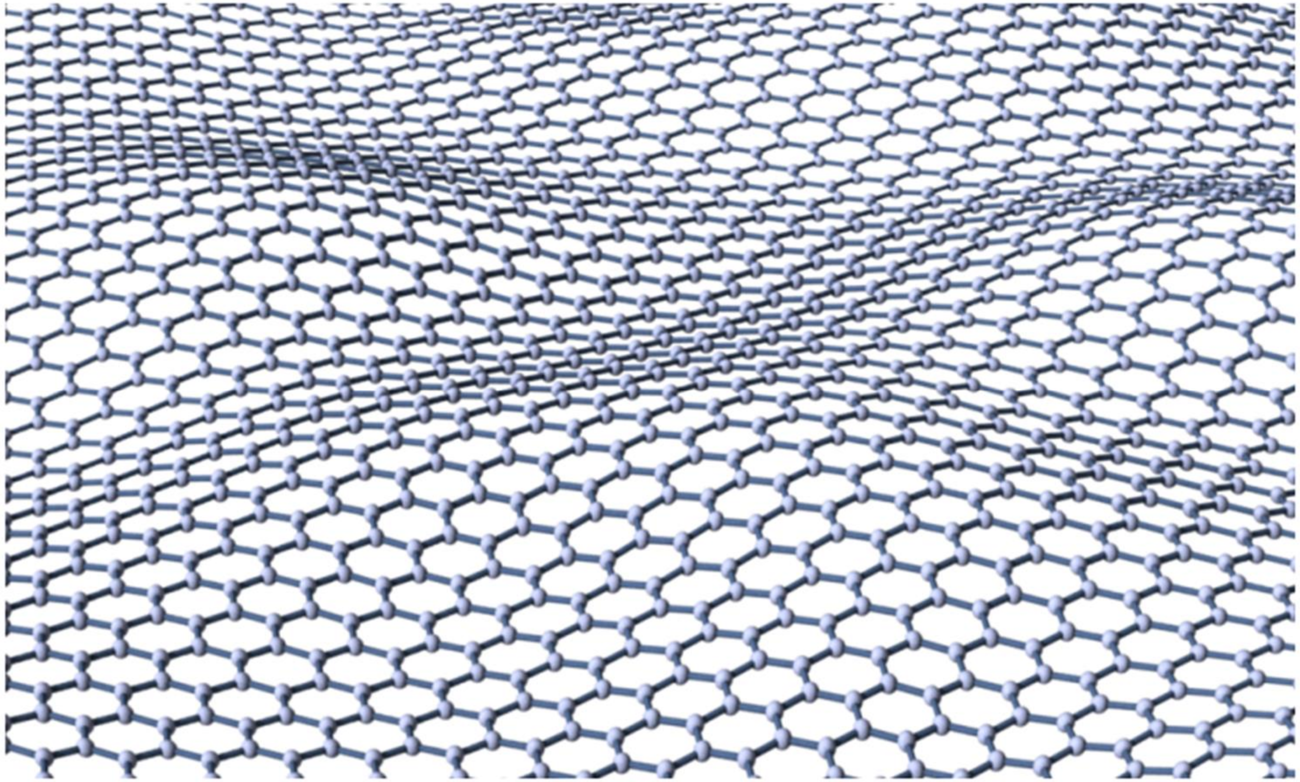

Can GIFAD give information about coupling of graphene with the substrate?

e.g. by using Moiré corrugation as a measure of graphene-substrate alignment and electronic transfer?

Alignment of graphene

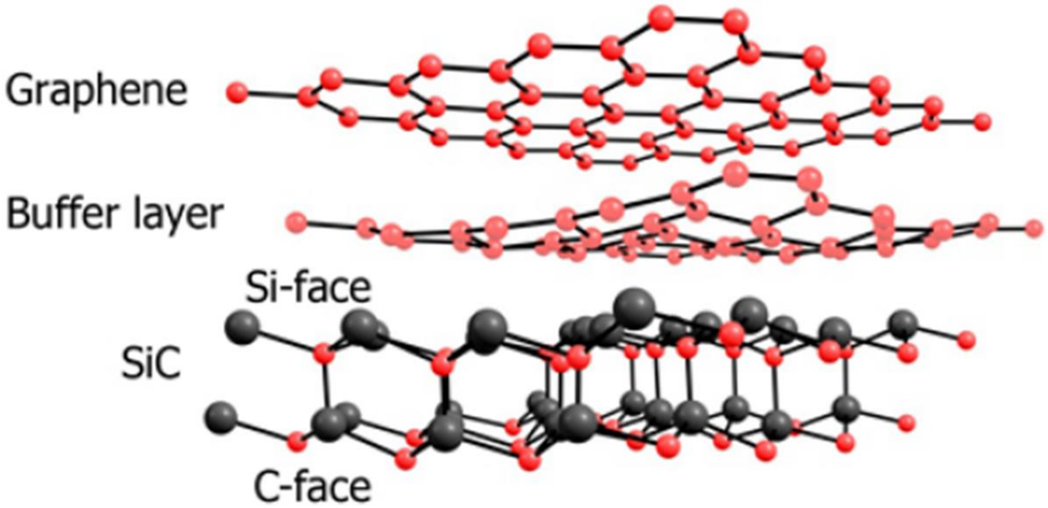

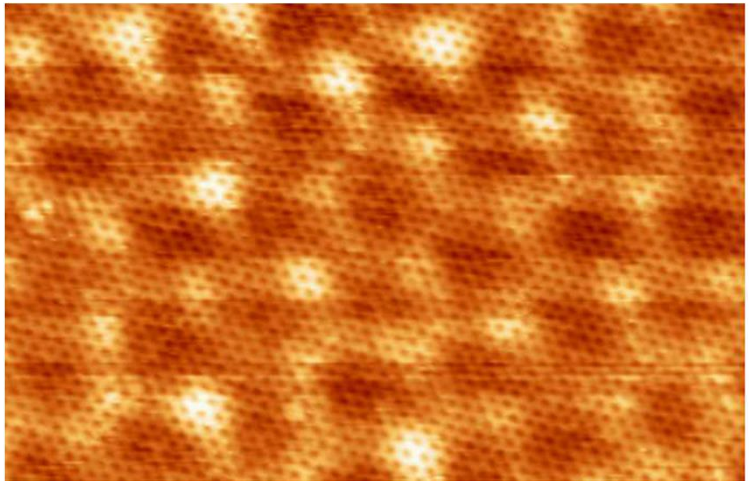

Growth of graphene on SiC(0001) substrate by annealing at 1325°C for 25 min

STM measurements show graphene modulated by LDOS of underlying buffer

GIFAD offers the possibility of extracting the same information, more rapidly, in real-time during growth, without tip convolution effects.

Alignment of graphene

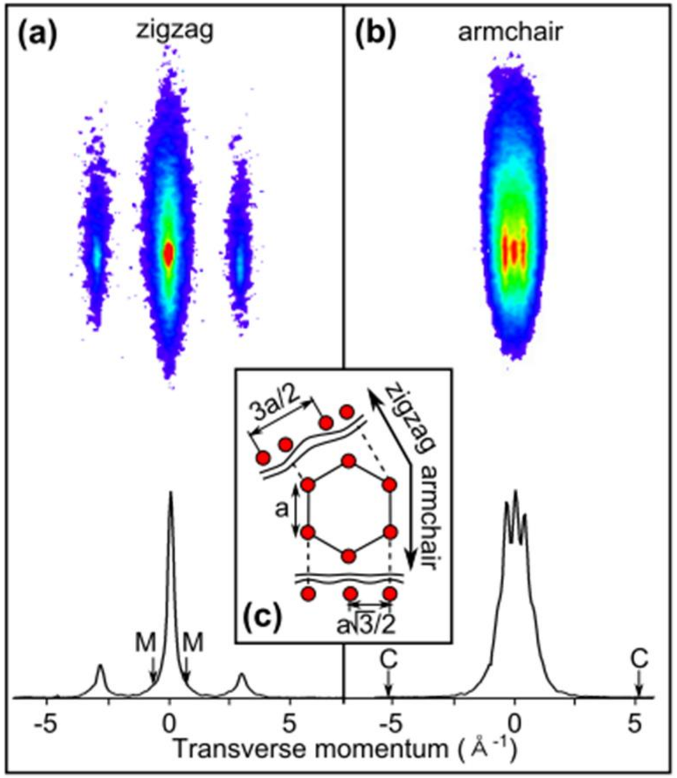

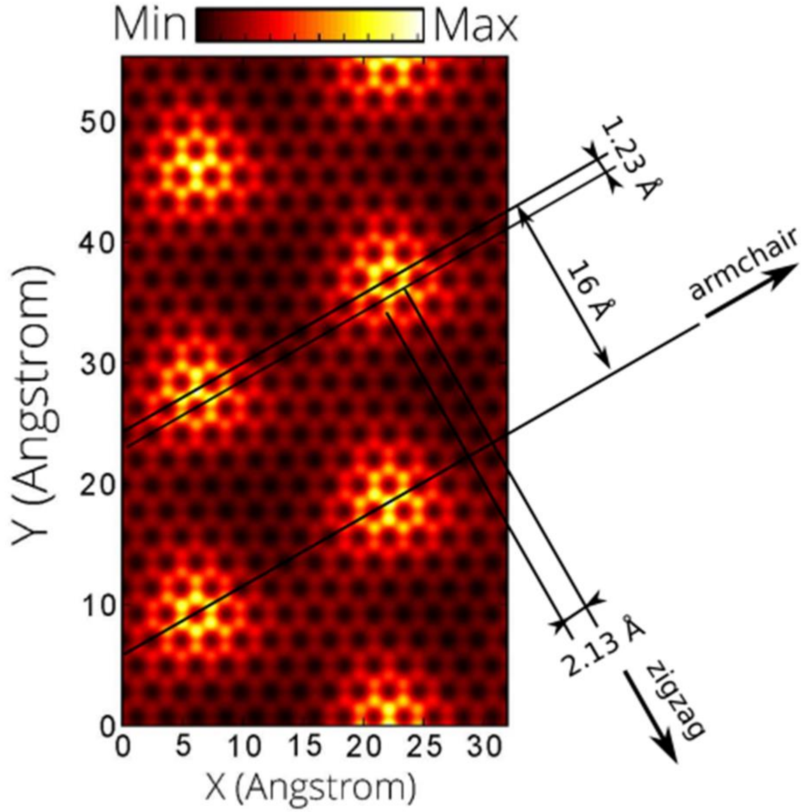

Å 2 channeling azimuthal directions identified separated by 30°

Å « zigzag » corresponds to the carbon structure : corrugation 0,007 Å

Å « armchair » corresponds to the Moiré superstructure : corrugation 0,07 Å

Å Corrugation found by comparing experiment with full quantum calculations

Zugarramurdi et al, APL, 106, 101902 (2015); Debiossac, PRB, 94, 205403 (2016)

Growth of organic molecular thin films

Want in-situ, non-destructive assessment of molecular organisation

GIFAD
- allows unit cell size and surface electronic density to be measured
- requires long range order
- requires lateral coherence length (Δ_x) < lattice parameter (d) where $\Delta_x = 2\pi/k_0\Delta\psi$

Atom beam triangulation
- allows identification of low index directions (channels) of the topmost layer
- [illegible] nit cell size

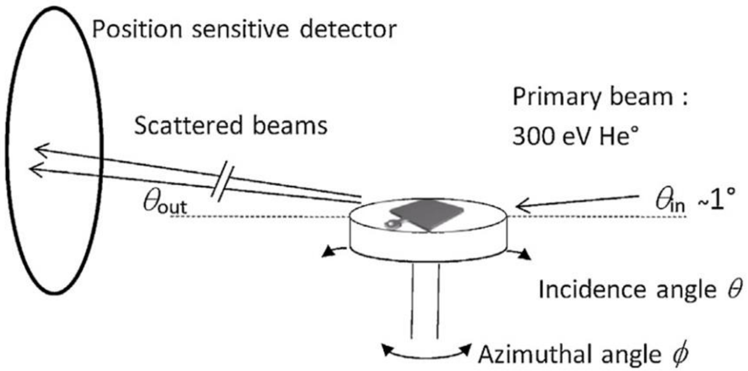

300 eV He
➔ E_Q ~ 50 – 100 meV
➔ minimum impact ~ 3 – 4 Å
(prevents penetration of molecular film
even in incomplete coverage
regime)

Growth of organic molecular thin films

Example: perylene monolayer on Ag (110)

Raw data | Polar transform

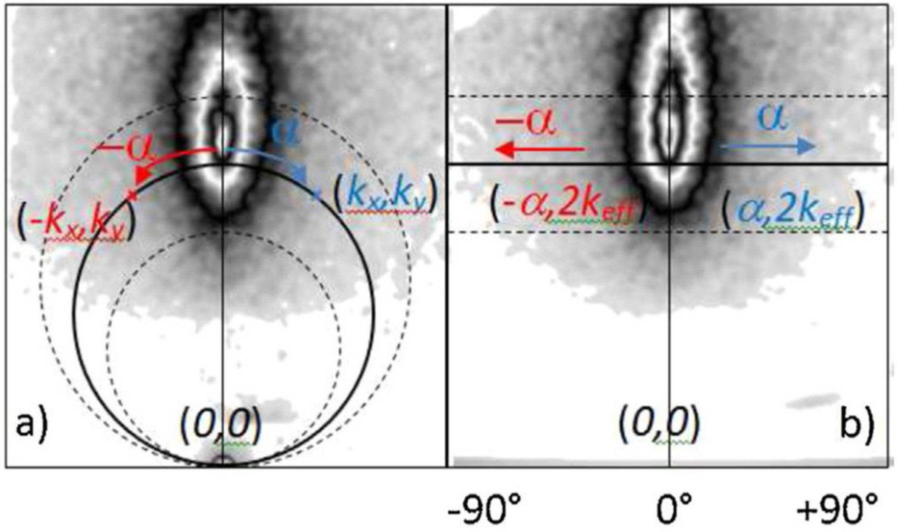

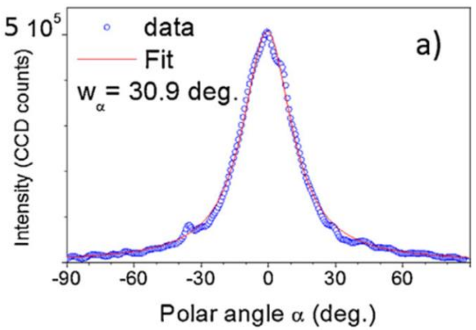

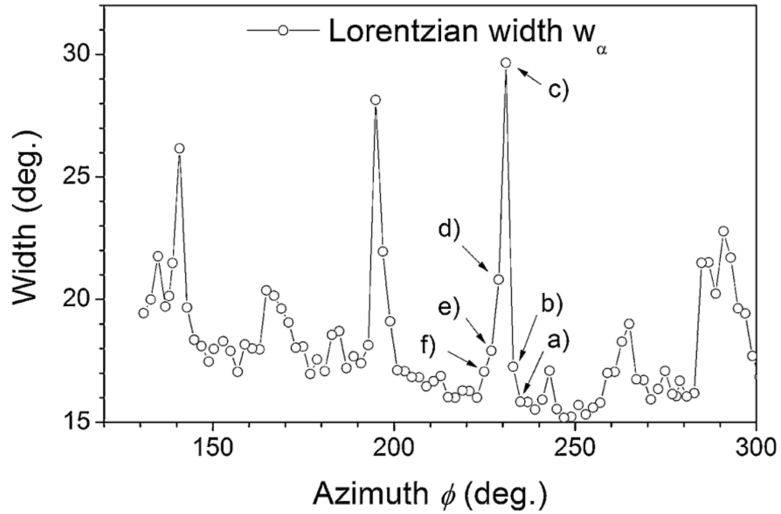

Ordering of molecules on surface
➔ peaks correspond to low index directions

Kalashnyk et al, Appl. Surf. Sci. 364, 235 (2016)

Growth of organic molecular thin films

Example: perylene monolayer on Ag (110)

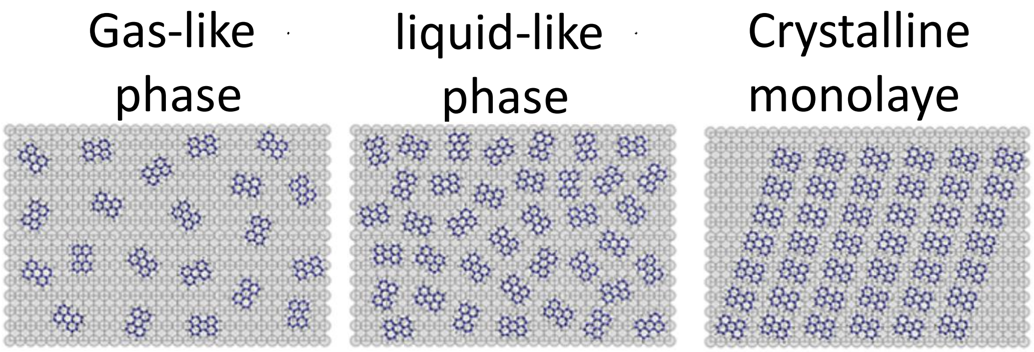

- Growth of a “wetting layer” followed by sharp change in reflectivity indicating a phase change
- Reflectivity curve independent of He beam conditions (energy, azimuth...)
- Decrease in sticking coefficient of perylene as coverage increases
- Increased desorption at phase change
- Kinks in mean exit angle indicate change in local organisation of molecules

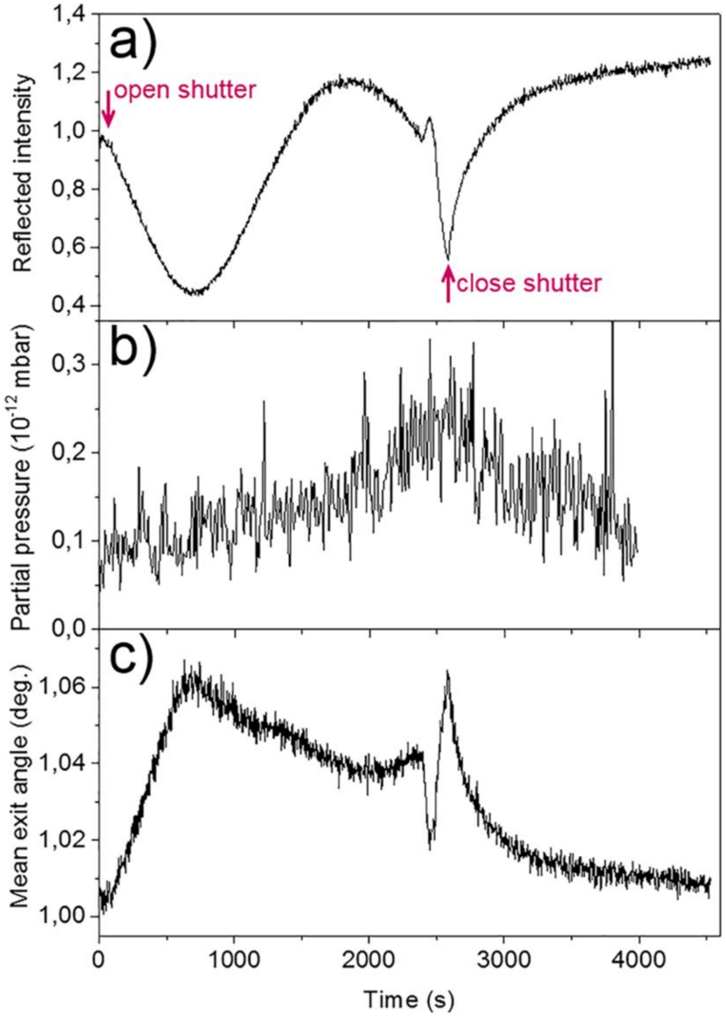

Momeni et al, J. Phys. Chem. Lett. 9,908 (2018)

Growth of organic molecular thin films

Example: perylene monolayer on Ag (110)

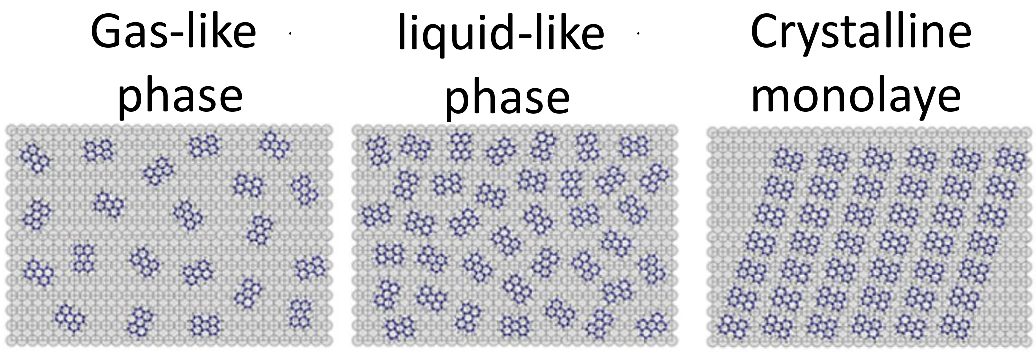

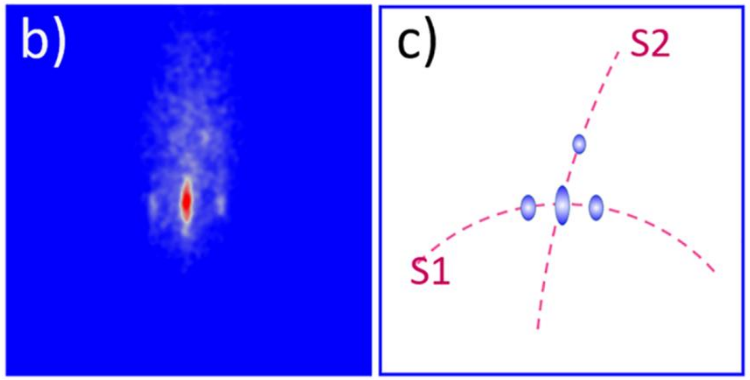

- Diffraction pattern shows two different crystal structures with different crystallographic orientations
- S2 crystallises before "monolayer" completion
- S1 crystallised after "monolayer" completion

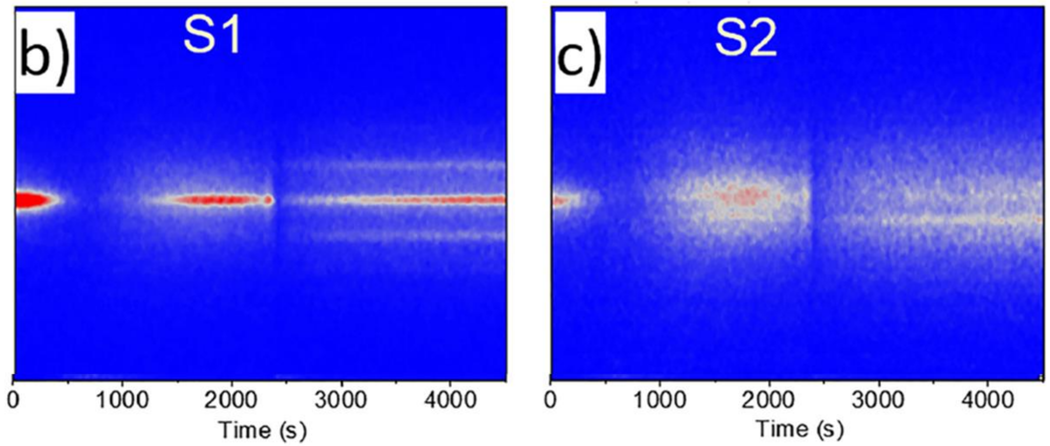

Momeni et al, J. Phys. Chem. Lett. 9,908 (2018)

Growth of organic molecular thin films

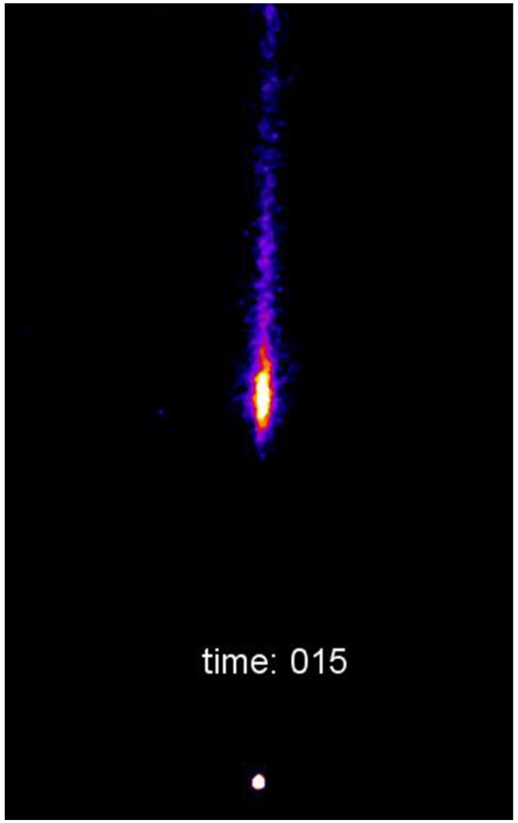

Video at :
https://pubs.acs.org/doi/suppl/10.1021/acs.jpclett.7b03246/suppl_file/jz7b03246_si_002.avi

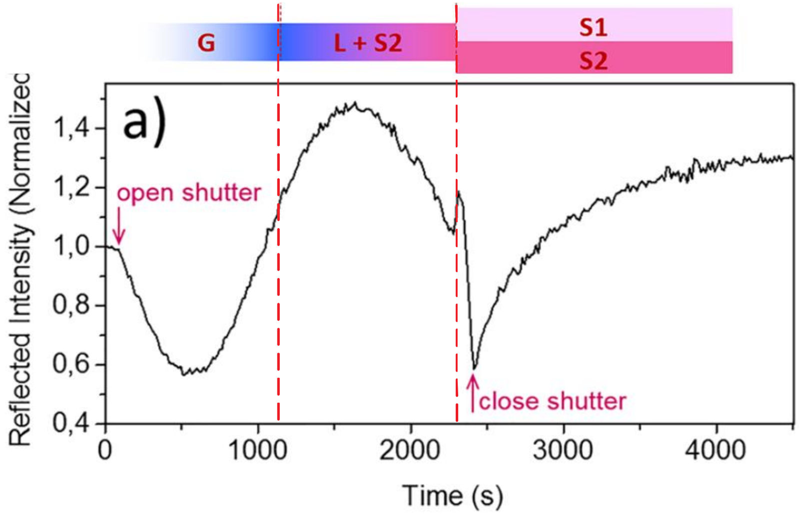

1) Initial growth – dilute phase of molecules lying flat on the substrate
2) Crystalline (S2) domains start to form in co-existence with liquid phase
3) At critical density: molecules tilt out-of-plane, First layer crystallises into compact (S1) structure

GIFAD can follow the dynamics of molecular thin film growth – crystallisation, changes in packing density and molecule orientation!

Momeni et al, J. Phys. Chem. Lett. 9,908 (2018)

Future perspectives

Take advantage of the chemical sensitivity of He-scattering to determine surface adatom composition

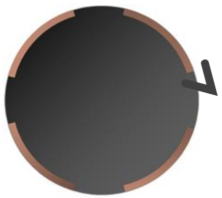

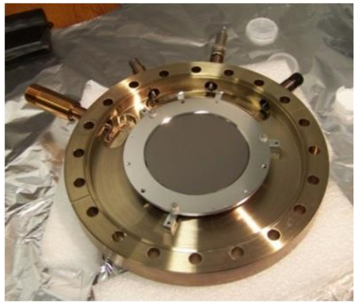

Undoped Si wafer with 4 Cu electrodes, and 2 MCP plates for time of flight position sensitive detection of recoil adatoms with pulsed He source

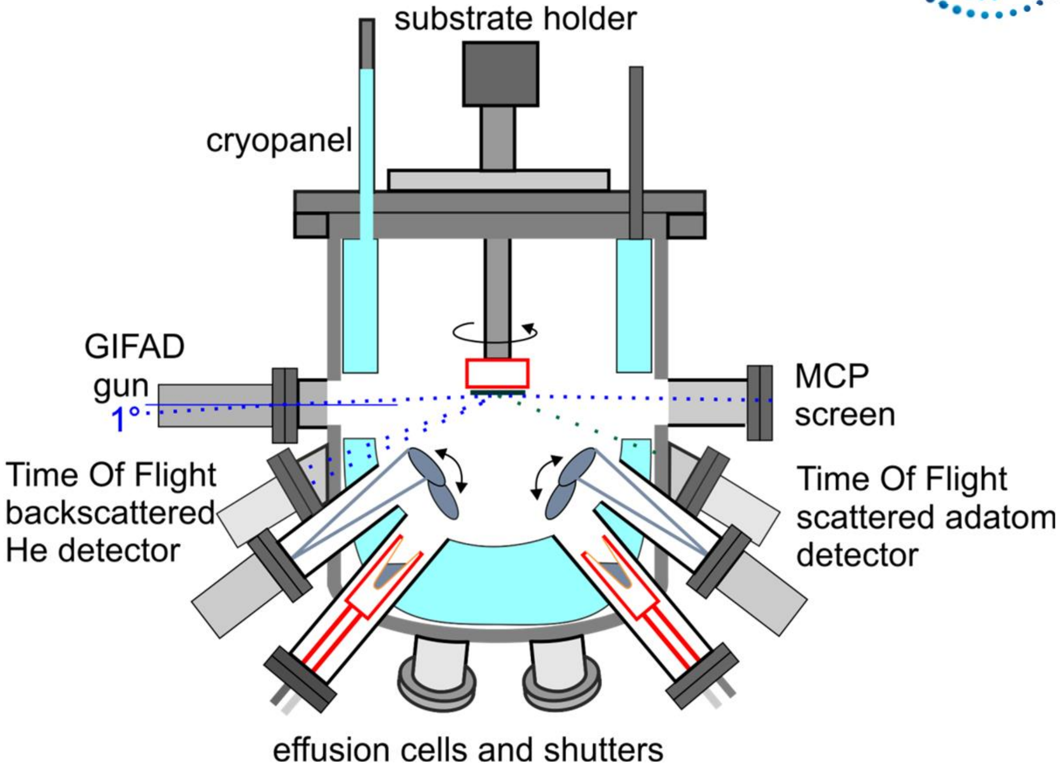

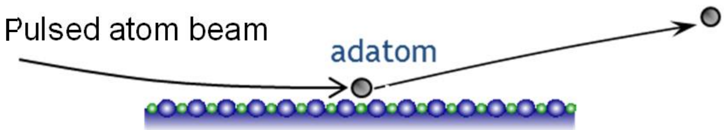

detection of ad-atoms ejected at large angle
⇒ identification of light elements (hydrogen)

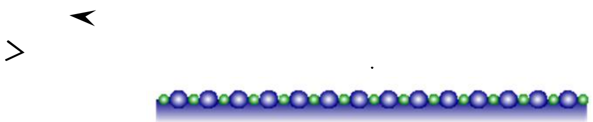

detection of atoms scattered at large angle (30°)
⇒ identification of heavy elements

Summary

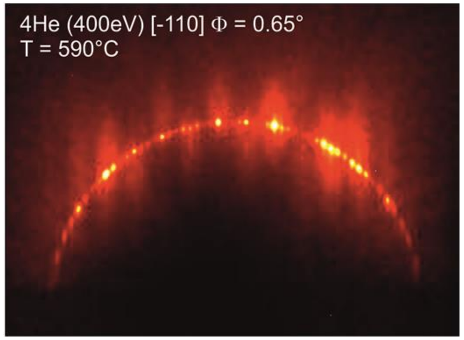
4He (400eV) [-110] Φ = 0.65°
T = 590°C

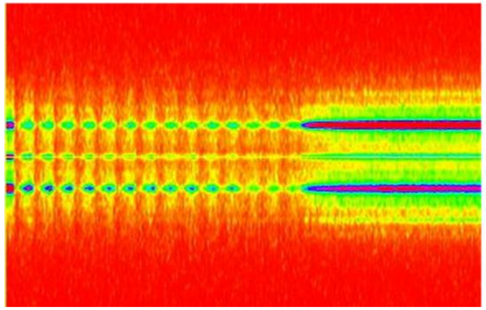

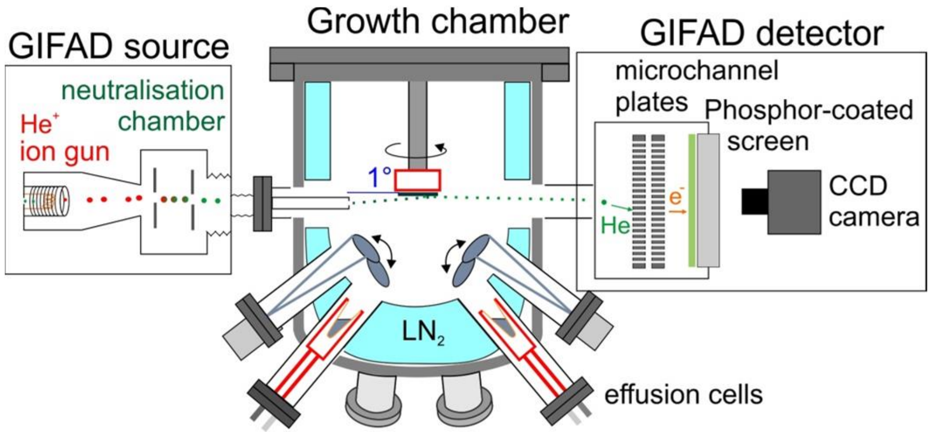
GIFAD source
neutralisation chamber
He+ ion gun
Growth chamber
1°
LN2
effusion cells
GIFAD detector
microchannel plates
Phosphor-coated screen
e-
He
CCD camera

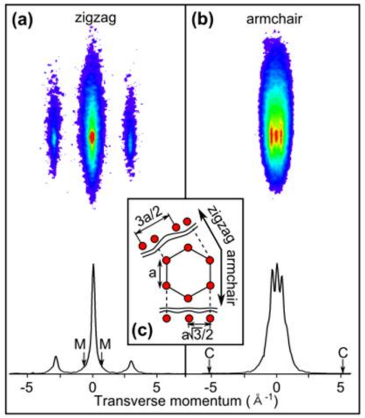
(a) zigzag
(b) armchair
(c)
3a/2
a
zigzag
armchair
a√3/2
M
M
C
C
-5
0
5
-5
0
5
Transverse momentum (Å-1)

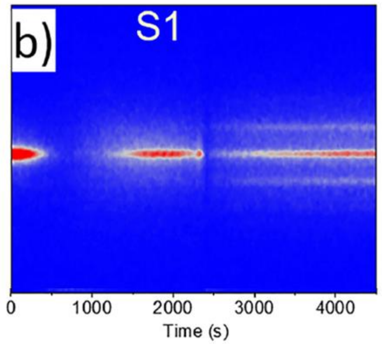
b)
S1
0
1000
2000
3000
4000
Time (s)

Additional useful references

H. Winter, « Collisions of atoms and ions with surfaces under grazing incidence » Physics Reports 367 387-582 (2002)

H. Winter and A. Schüller, « Fast atom diffraction during grazing scattering from surfaces » Progress in Surface Science, vol 86. pp 169-221 (2011)

Diffraction dôatomes rapides sur surfaces : des résonances de piégeage à la dynamique de croissance par épitaxie : PhD Thesis, Maxime Debiossac, (2014)
https://tel.archives-ouvertes.fr/tel-01128981

Collisions rasantes d'ions ou d'atomes sur les surfaces : de l'échange de charge à la diffraction atomique: PhD Thesis, Patrick Rousseau (2006)
https://tel.archives-ouvertes.fr/tel-00106727

Quanten-Regenbogenstreuung bei axialer Oberflächen-Gitterführung schneller Atome: PhD Thesis, Andreas Schüller (2010)
https://edoc.hu-berlin.de/handle/18452/16813

ISMO website, SIREN group:
http://www.ismo.u-psud.fr/spip.php?rubrique66 ,
http://www.ismo.u-psud.fr/spip.php?rubrique381